MEMORANDUM

From/De : Paula Bordalo, Eva-Maria Kabuß, Konrad Klimaszewski, Krzystof Kurek, Sérgio Ramos, Luís Silva, Marcin Stolarski.

To/à : COMPASS collaboration

Subject/Sujet : Determination of $\Delta G/G$ for $Q^2 > 1(\mathrm{GeV/c})^2$ from 2002-2006 high p_T data.

We present an evaluation of the gluon polarization $\Delta G/G$ for $Q^2 > 1(\mathrm{GeV/c})^2$ from high p_T hadron pair events collected in 2002-2006 years. A method based on Neural Network approach is described in details. The resulting value is $\Delta G/G = 0.125 \pm 0.060 \pm 0.065$ at averaged $x_G = 0.094$. Also a new result is given in 3 x_g bins

---

Contents

1 Determination of the gluon polarization $\Delta G/G$ for $Q^2 > 1(\mathbf{GeV/c})^2$.

1.1 Extraction of $\Delta G/G$ from measured asymmetries.

The helicity asymmetry for the production of two high-p_T hadrons in the large Q^2 regime, $Q^2 > 1(\mathrm{GeV/c})^2$, can be expressed as a function of x_{Bj} as follows:

$$A_{LL}^{2h}(x_{Bj}) = R_{PGF}\, a_{LL}^{PGF} \frac{\Delta G}{G}(x_G) + R_{LP}\, D\, A_1^{LO}(x_{Bj}) + R_{QCDC}\, a_{LL}^{QCDC} A_1^{LO}(x_C), \tag{1}$$

where

$$A_1^{LO} \equiv \frac{\sum_i e_i^2 \Delta q_i}{\sum_i e_i^2 q_i}, \tag{2}$$

and the R_i are the fractions of the sub-processes and the a_{LL}^i the so-called analyzing powers (the asymmetries of the partonic cross-sections). Labels LP, $QCDC$ and PGF refer to the different processes: leading order, *i.e.* photon absorption by quark; QCD Compton, *i.e.* gluon radiation by quark; and Photon-Gluon Fusion. D is the depolarization factor depending on y.

Evaluation of $\Delta G/G$ from equation (1) is possible only when the contribution from background processes (LP, QCDC) can be computed and subtracted. Therefore the analysis requires a precise Monte Carlo (MC) description of the data. The fractions R and the analyzing powers a_{LL} can be calculated using MC simulations based on the LEPTO generator [1]. There are two possibilities to estimate the A_1^{LO} asymmetry which is expressed in terms of polarized and unpolarized quarks distribution functions (PDF's). First, take the quarks distributions from polarized and unpolarized PDF's existing on the market, second use directly the measured inclusive A_1 asymmetry. In this analysis we use the second possibility which is less dependent on QCD analysis and related assumptions and approximations. Formula (1) is valid in Leading Order QCD approximation under several additional assumptions. First, independent fragmentation is assumed. This is not *à priori* the case in the MC simulation which uses JETSET [2], a string-type mechanism, to describe the fragmentation. However, MC studies performed with POLDIS [3] seem to justify this assumption. Next, we ignore the fact that the fragmentation functions are different for different flavors. This assumption is valid if only pions are produced and the kaon contamination in the high p_T sample is discussed in systematics. A possible spin-dependence of the fragmentation functions was estimated to be very small thus it is neglected. Finally, a linear dependence of $\Delta G/G$ in x_G is assumed in order to justify the substitution of the averaged value of $\Delta G/G$ with $\Delta G/G$ taken at average x_G. Although the shape of the gluon polarization is not known this assumption is always justified if x_G bins are small enough. For detailed discussion of the formula derivation see ref. [4].

The inclusive asymmetry A_{LL}^{incl} can also be decomposed in a similar way as in equation(1):

$$A_{LL}^{incl}(x_{Bj}) = R_{PGF}^{incl} a_{LL}^{incl,PGF} \frac{\Delta G}{G}(x_G) + R_{LP}^{incl} D A_1^{LO}(x_{Bj}) + R_{QCDC}^{incl} a_{LL}^{incl,QCDC} A_1^{LO}(x_C). \tag{3}$$

Note, that y, D, x_{Bj}, x_G and x_C in the inclusive and high p_T sample can be different. It was, however, checked in MC that the averaged x_G and x_C in the two samples are very similar, which simplifies the analysis.

Combining eqs (1) and (3) and neglecting small terms (note that the fractions R_{PGF} and R_{QCDC} are much smaller for the inclusive sample than for the high p_T sample) the formula for $\Delta G/G$ extraction reads:

$$\begin{aligned} A_{LL}^{2h}(x_{Bj}) &= R_{PGF} a_{LL}^{PGF} \frac{\Delta G}{G}(x_G) + \frac{R_{LP}}{R_{LP}^{incl}} D (A_1(x_{Bj}) - A_1(x_C) \frac{a_{LL}^{incl,QCDC}}{D} \frac{R_{QCDC}^{incl}}{R_{LP}^{incl}} - R_{PGF}^{incl} \frac{a_{LL}^{PGF}}{D} \frac{\Delta G}{G}(x_G)) \\ &+ \frac{R_{QCDC}}{R_{LP}^{incl}} a_{LL}^{QCDC} (A_1(x_C) - A_1(x'_C) \frac{a_{LL}^{incl,QCDC}}{D} \frac{R_{QCDC}^{incl}}{R_{LP}^{incl}} - R_{PGF}^{incl} \frac{a_{LL}^{PGF}}{D} \frac{\Delta G}{G}(x'_G)) \end{aligned} \tag{4}$$

where

$$A_1(x) = \frac{A_{LL}^{incl}}{D} \tag{5}$$

Due to the fact that $\Delta G/G$ is present in formula (4) at two different x_G (noted x_G and x'_G), the extraction of $\Delta G/G$ requires a new definition of the averaged x_G at which the measurement is performed:

$$x_G^{av} = \frac{\alpha_1 x_G - \alpha_2 x'_G}{\beta} \tag{6}$$

where:

$$\alpha_1 = a_{LL}^{PGF} R_{PGF} - a_{LL}^{incl,PGF} R_{LP} \frac{R_{PGF}^{incl}}{R_{LP}^{incl}} \tag{7}$$

$$\alpha_2 = a_{LL}^{incl,PGF} R_{QCDC} \frac{R_{PGF}^{incl}}{R_{LP}^{incl}} \frac{a_{LL}^{QCDC}}{D} \tag{8}$$

$$\beta = \alpha_1 - \alpha_2. \tag{9}$$

This definition relies on the assumption of a linear dependence of $\Delta G/G$ upon x_G; this assumption is justified for every shape of $\Delta G/G$ if bins in x_G are not too wide.

The final formula for the gluon polarization can now be written as follows:

$$\begin{aligned} \Delta G/G(x_G^{av}) &= \frac{A_{LL}^{2h}(x_{Bj}) + A^{corr}}{\beta} \\ A^{corr} &= -A_1(x_{Bj}) D \frac{R_{LP}}{R_{LP}^{incl}} - A_1(x_C)\beta_1 + A_1(x'_C)\beta_2 \end{aligned} \tag{10}$$

and

$$\begin{aligned} \beta_1 &= \frac{1}{R_{LP}^{incl}} (a_{LL}^{QCDC} R_{QCDC} - a_{LL}^{incl,QCDC} R_{QCDC}^{incl} \frac{R_{LP}}{R_{LP}^{incl}}) \\ \beta_2 &= a_{LL}^{incl,QCDC} \frac{R_{QCDC}^{incl}}{R_{LP}^{incl}} \frac{R_{QCDC}}{R_{LP}^{incl}} \frac{a_{LL}^{QCDC}}{D} \end{aligned} \tag{11}$$

Measured asymmetries are related to the A_{LL}^{2h} in standard way with weight fP_TP_B. The coefficients in A^{corr} asymmetry: β_1, β_2 as well as β are estimated using high p_T MC sample and inclusive MC sample. Also x_C and x_G^{av} are estimated from MC. As it is written in next sections - the Neural Network parametrization is used event by event.

1.2 High p_T cuts method and Neural Network approach.

The original idea of high p_T analysis was to suppress the contribution of the dominant LP process by requiring the presence of two hadrons with high transverse momenta. However, removing the LP process would require to select only very high p_T, which would result in a dramatic loss of statistics. A compromise has to be found, and in practice our sample will include significant contributions from the three processes, which has to be taken into account in the extraction of $\Delta G/G$.

The analyzes performed in SMC [5] and in COMPASS [6], [7] were using selections of events optimized to obtain high PGF contributions and they made simplifying assumptions in the formulae for $\Delta G/G$ extraction. In the SMC analysis two alternative selections were used: a cut on $\Sigma p_T^2 > 2.5(\mathrm{GeV}/c)^2$ dramatically reduced the statistics while a neural network selection was less restrictive, but the final sample was of the order of 50,000 events only. In the determination of the gluon polarization the contributions of LP and QCD Compton processes to the measured asymmetry were estimated neglecting the difference in the parton momentum fraction probed in these two processes and the measured A_1 was used as an approximation for the quark distribution ratio ($A_1 \simeq A_1^{LO}$).

In COMPASS the first analysis also used a cut on $\Sigma p_T^2 > 2.5(\mathrm{GeV/c})^2$. In a second analysis the cuts were optimized on the error on $\Delta G/G$ rather than on the PGF fraction, leading to a cut $\Sigma p_T^2 > 1.3(\mathrm{GeV/c})^2$, but this result was not released. In the gluon polarization extraction again the quark asymmetries were estimated by measured inclusive asymmetry A_1, taken at the same $x \simeq x_{Bj}$ for LP and QCD Compton processes. As a consequence the contribution of these processes to the measured asymmetry was completely neglected due to the fact that the inclusive A_1 asymmetry is close to zero at the averaged x_{Bj} of the selected data sample.

Such simplifications can no longer be justified with the statistical precision now accessible. In the present analysis a special effort was made to treat the contributions from all processes as precisely as possible. The derivations of the formulae are given in the first section of this note. The final result will not be affected by the approximations.

A Neural Network (NN) was already used in the SMC analysis [5], where it was a tool for selecting PGF sub-processes from data sample. The NN was trained on a MC sample and then an optimized cut on NN response was used instead of the standard Σp_T^2 cut. It was shown that the NN selection is more effective than the $\Sigma p_T^2 > 2.5(\mathrm{GeV}/c)^2$ cut : it provides higher statistics for a given fraction of PGF or alternatively a larger PGF fraction for a given statistics. The improvement is not so obvious with respect to the $1.3(\mathrm{GeV/c})^2$ cut. A detailed description of the NN used for the selection of PGF events and of its application in SMC and COMPASS analyzes can be found in [8].

In the present analysis a NN is also used, but in a new way. No cut on NN response is used. The NN is assigning to each event a probability of originating from each of the three processes. The statistical weights constructed for each individual event include these probabilities. We do not have to remove events which most likely are not PGF, we can keep them and the weights will reduce their importance in the gluon polarization calculation. Such an approach makes the best use of the statistical power of the available data and it avoids a bias which can be introduced in the previous method due to the correlation of the analyzing power and the kinematic variables used in asymmetry determination.

The weight elements are of course related to the fractions, analyzing powers, x_G, x_C etc, according to the final formulas for $\Delta G/G$ extraction: (10) and (11). The different NN used in the present analysis provide not only probabilities of the three processes, but also the other elements needed for weight construction.

1.3 Weighting and $\Delta G/G$ extraction.

In the old method Eq. (10) was used to extract $\Delta G/G$ from the measured asymmetry, $A_{LL}^{2h}(x_{Bj})$, computed with weight $w_{old} = fDP_b$, which is the standard weight in several COMPASS analyzes. The terms A^{corr} and β were calculated only once using the mean values of all required variables, $A_1(\langle x_{Bj}\rangle)$, $\langle D\rangle$, $\frac{\langle R_{LP}\rangle}{\langle R_{LP}^{incl}\rangle}$ and so forth. As most of these variables are correlated with the weight[1] this results in a statistical bias [9]. To avoid it one can give up event weighing, which means a significant loss in figure of merit, or use a correct weight. In this analysis the latter option was chosen.

Following Ref. [9] the correct weight for high p_T analysis is $fDP_b\beta$ and A^{corr} has to be calculated on an event by event basis. This means that for every event we have to know:

- R_{PGF}, R_{QCDC}, R_{LP}
- R_{PGF}^{incl}, R_{QCDC}^{incl}, R_{LP}^{incl}
- a_{LL}^{PGF}, a_{LL}^{QCDC}
- $a_{LL}^{incl,PGF}$, $a_{LL}^{incl,QCDC}$

[1] In the above example *e.g.* mean value of the depolarization factor is used, which is also part of the weight used for $A_{LL}^{2h}(Xbj)$ calculation.

- $x_C,\ x_G$
- $f,\ D,\ P_b$

Within the above variables only those in the last line can be obtained from the data. The rest of them has to be estimated using a NN trained on a MC sample.

The 2^{nd} order asymmetry-extraction method [10] is used to extract $\Delta G/G$. The original equation (67) in [10] is modified to take into account the existence of a polarized background in the high p_T analysis, *i.e.* the A^{corr} term. The modified equation (67) reads

$$\delta = \frac{p_u p'_d}{p'_u p_d} = \frac{(C_u + <\beta_u>_w <\Delta G/G>)(C'_d + <\beta'_d>_w <\Delta G/G>)}{(C'_u + <\beta_{u'}>_w <\Delta G/G>)(C_d + <\beta_d>_w <\Delta G/G>)}, \tag{12}$$

where:

- $p_u = \sum_{i=0}^{N_i} w_i^u$,
- $<\beta_u>_w = \sum_{i=0}^{N_i} w_i^u (w_i^u P_t^u) / \sum_{i=0}^{N_i} w_i^u$,
- $C_u = 1 - \sum_{i=0}^{N_i} A_i^{corr} w_i^u / \sum_{i=0}^{N_i} w_i^u$.

and similar formulas for u', d and d'. In the original equation (67) the C terms were equal to 1. Note that comparing to the previous method we directly extract the value of $\Delta G/G$ without going through the intermediate step of extracting the $A_{LL}^{2h}(x_{Bj})$ asymmetry (the same happens in the open charm analysis).

1.3.1 NN training and its results

Several NN are used. They have a set of input parameters and are designed to provide a parametrization of a given quantity X. They are trained in a mode where the output is the expectation value of X for the considered values of the input parameters [2].

For the inclusive sample the input-parameter phase-space is x_{Bj} and Q^2, while for high p_T sample the transverse and longitudinal momenta of the hadron, p_{T1}, p_{T2}, p_{l1}, and p_{l2}, are used in addition. Note that, to avoid the bias discussed in the previous section, it is enough to know the mean value of all required variables in a selected phase-space point [3]. If the correlation between the NN output and the true value of X is not perfect, or even close to zero, the figure of merit is reduced but no bias is introduced.

The NN result for the parametrization of a_{LL}^{PGF}, a_{LL}^{QCDC}, $a_{LL}^{incl,PGF}$, $a_{LL}^{incl,QCDC}$, x_C, and x_G are presented in Fig. 1. The basic observation, which is still not understood, is that there is a good correlation for the a_{LL} for PGF's process and a poor one for QCDC process. It seems that for QCDC a_{LL} does not depend significantly upon any of the six input variables. This is even more surprising since the correlation for x_C and x_G are very similar and so are the values of x_C and x_G at a given phase-space point.

The example of Rs parametrization in 2 dimensional plots as a function of (p_T1, p_T2), (p_l1, p_l2) and (x_{Bj}, Q^2) *i.e.* all input variables is shown in Figure 2. Each time four out of six parameters are fixed in the NN input $x_{Bj} = 0.012$, $Q^2 = 2.2$ GeV^2, $pT1 = 1.4$ GeV, $pT2 = 0.8$ GeV $pl1 = 30$ GeV and $pl2 = 18$ GeV. These are the weighted mean values of our sample. As expected the higher value of transverse momentum of the hadrons the LP contribution to the sample is reduced while contribution of QCDC and PGF are enhanced. It looks like the that PGF slightly prefers symmetric pl1 and pl2. Finally on the (x, Q^2) plot one can observe that the fraction of PGF is very small for high x_{Bj} region in addition QCDC dominates at high value of y, while LP is concentrated on lower values of it. More details about systematic stability of NN are discussed in sections: 5.5 and 5.6.

2 Data sample and event selection.

The data sample used includes data from the years 2002, 2003, 2004 and 2006 years. Selected events have a primary vertex containing a beam muon, a scattered muon and at least two hadrons with high transverse momentum. The primary vertex is identified using `BestPrimaryVertex()` provided by PHAST [11].

[2] technically this means that the error calculated during NN training has to be a standard $\sum_i (X_{in} - X_{out})^2$, the neuron(s) of the last layer (output layer) has to work in the linear mode *i.e.* output signal of the neuron is proportional to the amplitudes of the input signals.

[3] the extreme example is a non-weighted method, where variables are averaged over the whole phase space and the final result is not biased. The problem starts if the variables are correlated and averaged over different phase spaces.

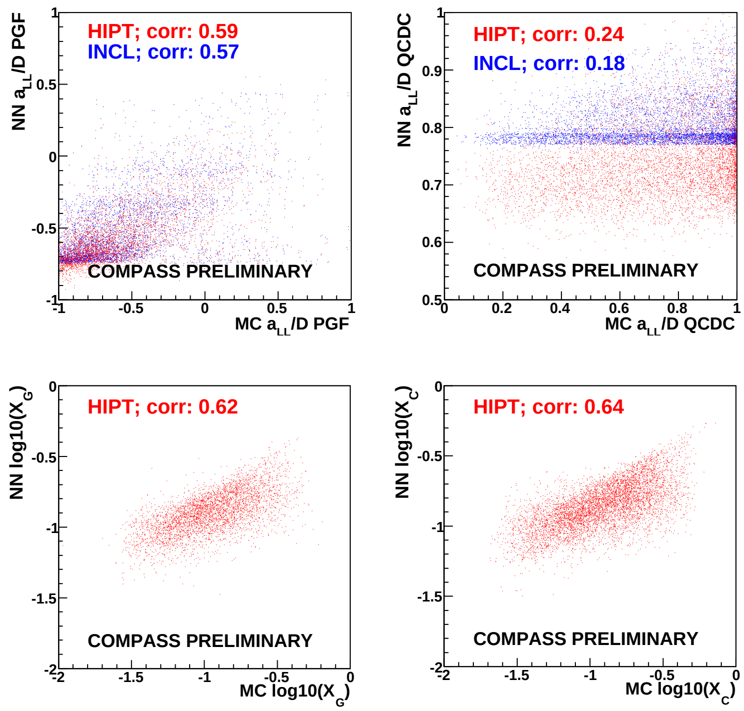

Figure 1: Output of NN for $a'_{LL}s$ and $x's$. See text for details.

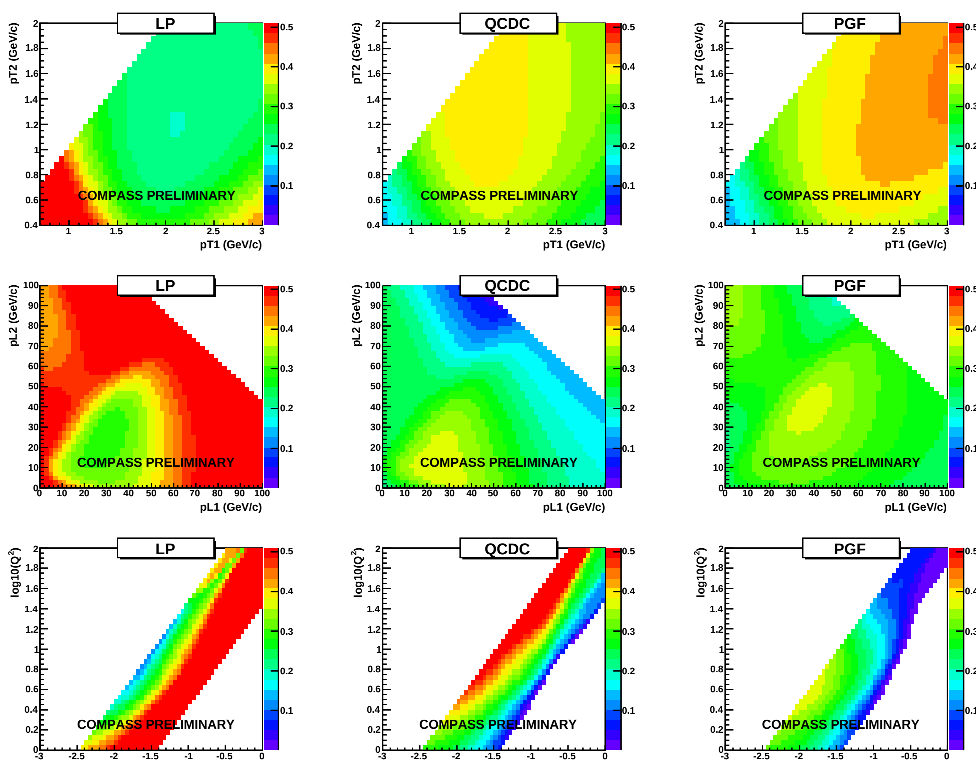

Figure 2: Output of NN for $a'_{LL}s$ and $x's$. See text for details.

Figure 3: The longitudinal vertex distribution (left) with the cuts along z coord.($-100\ cm < z < -40\ cm$ and $-30\ cm < z < 30\ cm$) and the transverse vertex distribution (right) with cuts on $y > 1\ cm$ and $r < 1.3\ cm$

To calculate $\Delta G/G$ for a given data taking period, runs with positive and negative orientations of solenoid field are combined in a *consecutive* way. A disagreement with *global* configuration was observed in several cases for 2006 data sample. After thorough study it was traced to instabilities of the spectrometer. Therefore the *consecutive* configuration was selected as offering better reduction of instabilities. The runs were grouped into configurations according to the official "grouping lists" [12]. The periods and production slots are shown in Table 1. During data selection, events were removed according to the *badspill* lists defined in [12].

Period	Slot	Period	Slot	Period	Slot
02P1C	2	03P1J	3	06W32	2
02P2A	3	04W22	2	06W33	2
02P2D	3	04W23	3	06W34	2
02P2E	2	04W26	2	06W35	2
02P2F	2	04W27	2	06W36	2
02P2G	2	04W28	2	06W37	2
02P3G	2	04W29	1	06W40	2
03P1A	2	04W30	2	06W41	2
03P1B	2	04W31	2	06W42	2
03P1C	3	04W32	3	06W43	2
03P1D	2	04W37	1	06W44	2
03P1E	2	04W38	3	06W45	2
03P1F	2	04W39	3	06W46	3
03P1I	2	04W40	3		

Table 1: Periods and slots.

2.1 Target geometry

The incoming muon, μ, is required to cross both target cells and the primary vertex to be inside the nominal target volume. These two conditions are ensured by using the PHAST functions `CrossCells()` and `InTarget()`, respectively, with a radius $r < 1.3\ cm$ and $y < 1.0\ cm$ ($r < 1.3\ cm$ and $y < 1.3\ cm$) for 2002-04 (2006) data sample. Figure 3 shows the longitudinal and transverse vertex distributions, together with related cuts.

2.2 Particle identification

The scattered muon, μ', is identified using the functions `IsMuPrim()` and `iMuPrim()` from PHAST (version 7.102). The main requirement for a particle to be a μ' [13] is that it had traveled through enough material to be safely considered as a muon, and for that purpose a $X/X_0 > 30$ cut is used on the number of radiation lengths overtaken. To clean up the sample the μ' candidate is required to travel through the active area of one of the triggers that fired for a considered event. In addition if the primary vertex contains more than one scattered muon the event is rejected. Finally events are rejected in case there is a high momentum hadron track that traveled through absorber beam hole as it could be the real μ'. In case of semi-inclusive triggers it is required that there is at least one hadron track in the primary vertex.

The two particles with highest p_T associated with the primary vertex besides μ and μ' are considered as *hadron candidates*. They must fulfill the following requirements:

- The hadron candidates are not muons. There is indeed a small probability for a pile-up muon to be included in the primary vertex and therefore being considered as a hadron candidate. The hadron candidate is rejected if it traveled through too much material ($X/X_0 > 30$) or if it goes through the Muon Filter 2 (position of the last cluster $z > 40\ m$).

- The track reconstruction quality is good. First, $\chi^2/ndf < 20$. Then, it is verified that the track was not reconstructed only within the fringe field of SM1 by requiring the last cluster to be located behind SM1.

- Hadrons do not go through the solenoid. The hadron tracks are extrapolated to the entrance of the solenoid and then the distance between the track and the z axis should be less than the radius of the solenoid aperture ($R = 14.9\ cm$, $Z = 118.4\ cm$ for 2002-04 and $R = 35.0\ cm$, $Z = 130.5\ cm$ for 2006).

2.3 Cuts on inclusive kinematic variables

- $Q^2 > 1$ (GeV/c)^2. Unsure that we select events from perturbative region.
- $0.1 < y < 0.9$. Events with $y < 0.1$ are rejected because their depolarization factor is rather low, while events with $y > 0.9$ are rejected because they are strongly affected by radiative effects, which are difficult to evaluate.

2.4 Cuts on hadronic kinematics variables

The following cuts are applied to the leading (highest transverse momentum) and next-to-leading hadrons:

- $p_{T1} > 0.7$ GeV/c and $p_{T2} > 0.4$ GeV/c. The cut for leading hadron remains as in previous analyzes. Due to the event weighting the cut on the second hadron was lowered in order to increase the statistics. The introduced background events will be suppressed by smaller weights. This requirement constitutes the *high* p_T cut.
- $z_1 + z_2 < 0.95$. Reject events from exclusive production.
- $x_F > 0$. Select current fragmentation region.

The number of events and the percentage that survives each cut are displayed in the Table 2. As a starting point for the selection a micro DST produced by Luis was used. It contains events selected with following cuts:

- Identified primary vertex, μ and μ'
- $Q^2 > 0.7$ GeV/c^2
- $p_{T1} > 0.35$ GeV/c, $p_{T2} > 0.35$ GeV/c
- Bad spill and run lists

In the table there are a few technical cuts that require some words of explanation:

- "Ineffective region of MT" - a region of Middle Trigger acceptance was found to be ineffective in 2006. It was decided to remove events with μ' reconstructed in that region. The inefficiency was not stable and varied in time in addition it affected comparison with MC (*c.f.* section 3.1).
- "Grouping cut" - events that do not belong to a group of runs defined in grouping lists are rejected.
- "Solenoid > 100 A" - field rotation runs are rejected due to uncertainties in the solenoid current evaluation.
- "Empty configurations" - Configurations where all events were rejected by other cuts are removed. This happens only in few cases for 2006 data.

The distributions of the kinematic variables Q^2, y, x_{Bj} are shown in fig. 4. Figs. 5 and 6 present the distributions of p, p_T, $\sum p_T^2$ and z variables for the leading and sub-leading hadrons.

3 Monte Carlo simulation and comparison with data.

This section focus on the MC simulation system. The description of the apparatus and the physical aspects of the present analysis concerning MC tuning, at the generation level, will be discussed. Finally the comparison between data and MC is presented.

Cuts	2002		2003		2004		2006		All years	
	# Events	%	# Events	%	# Events	%	# Events	%	# Events	%
micro DST	9146075	100.00	19002305	100.00	38253588	100.00	36697956	100.00	103099924	100.00
≥ 4 particles in event	7606575	83.17	16640796	87.57	35031752	91.58	34531980	94.10	93811103	90.99
Ineffective region of MT	7606575	83.17	16640796	87.57	35031752	91.58	33801539	92.11	93080662	90.28
Target cuts	4730494	51.72	10640710	56.00	23080442	60.34	21718149	59.18	60169795	58.36
$Q^2 > 1$ GeV/c^2	3364874	36.79	7921287	41.69	17193086	44.95	16419888	44.74	44899135	43.55
$0.1 < y < 0.9$	3133251	34.26	7289299	38.36	15624721	40.85	14794021	40.31	40841292	39.61
≥ 2 outgoing hadrons	2179813	23.83	5188411	27.30	10470930	27.37	12561232	34.23	30400386	29.49
p_T cut	685527	7.50	1672704	8.80	3374947	8.82	4654945	12.68	10388123	10.08
Hadron χ^2 cut	685523	7.50	1672695	8.80	3374872	8.82	4654340	12.68	10387430	10.08
Solenoid aperture cut	604283	6.61	1470687	7.74	2956183	7.73	4620795	12.59	9651948	9.36
Grouping cut	470268	5.14	1431545	7.53	2902851	7.59	3962690	10.80	8767354	8.50
Solenoid > 100 A	470268	5.14	1431545	7.53	2896501	7.57	3934698	10.72	8733012	8.47
Hadron ID	468404	5.12	1425748	7.50	2884986	7.54	3925816	10.70	8704954	8.44
$x_F > 0$	462642	5.06	1402413	7.38	2841504	7.43	2868271	7.82	7574830	7.35
$z_1 + z_2 < 0.95$	455612	4.98	1385086	7.29	2805543	7.33	2834678	7.72	7480919	7.26
SM1 fringe field	450134	4.92	1363630	7.18	2770995	7.24	2776831	7.57	7361590	7.14
Empty configurations	450134	4.92	1363630	7.18	2770995	7.24	2722176	7.42	7306935	7.09

Table 2: Table summarizing cuts. Lines correspond to relevant cuts and present the number (fraction) of events that survived the cut.

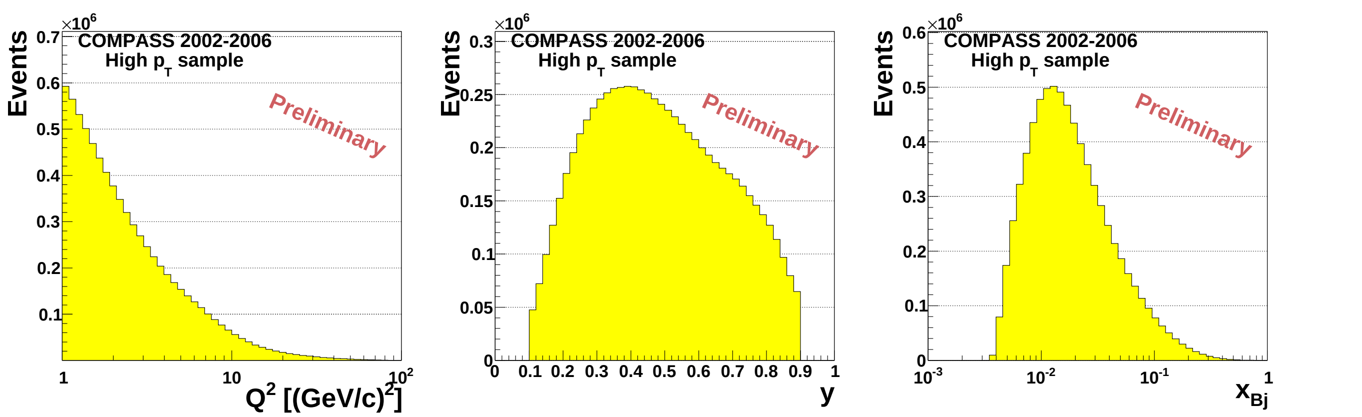

Figure 4: Q^2, y and x distributions

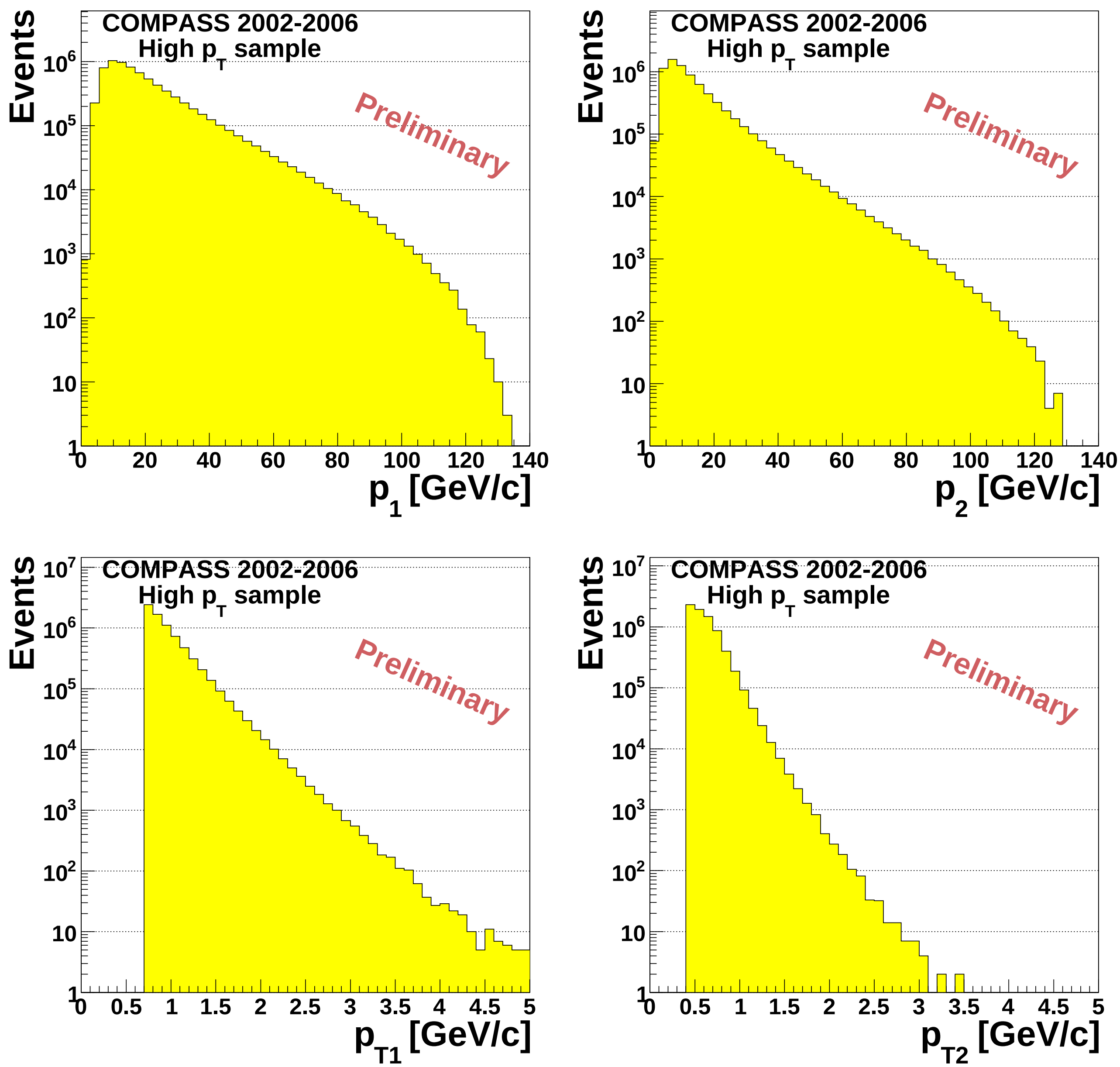

Figure 5: p and p_T for leading and sub-leading hadrons: The left column shows the leading hadrons and the right column the sub-leading one. In the first row the momenta are plotted, in the second row the transverse momenta are shown.

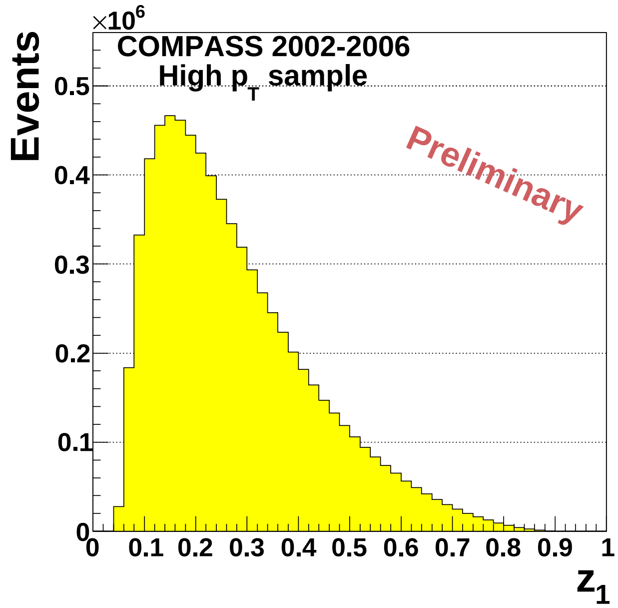

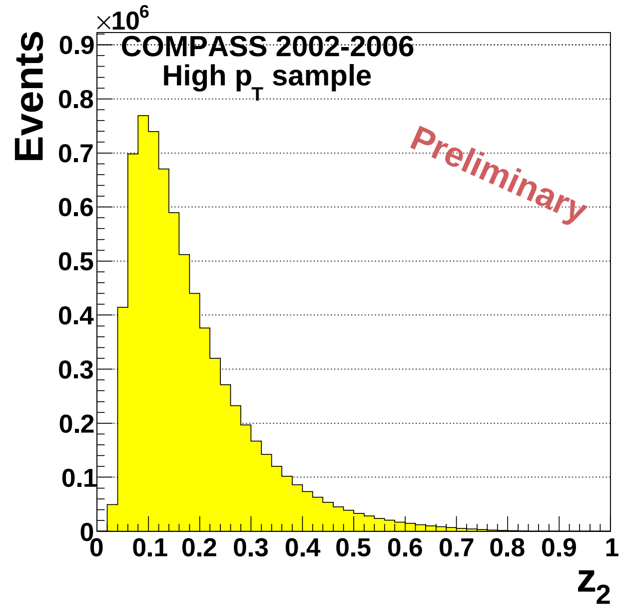

Figure 6: The distributions of the fraction of energy taken by the leading (left) and the sub-leading hadron (right) are shown.

3.1 MC simulations and improvement of the apparatus description.

Many characteristics of the sample essential for the extraction of the gluon polarization have to be obtained from the Monte Carlo simulations. In order to be available on event-by-event basis they are parametrized using Neural Networks (Sec. 1.2). This is the reason why a good description of the experimental data by MC is crucial for the analysis. In order to compute the weights needed for the extraction of $\Delta G/G$ we need information from two samples: the selected "high p_T" sample and the inclusive one. Both samples should be restricted to DIS region, defined here by $Q^2 > 1\,(\mathrm{GeV/c})^2$. All events surviving cuts listed below are kept for the inclusive sample, and to the high p_T MC sample the same cuts are applied as in the analysis of the experimental data.

In principle both samples should be generated in several sets each prepared to describe one year of data taking. In practice only two sets are used: one generated using the 2004 spectrometer setup and the second using the 2006 geometry. The 2004 data represent the majority of the data sample collected in the 2002-2004 period. In addition this data sample is the most complete from phase-space point of view for the considered period and it was shown [14] that 2004 MC gives satisfactory description of 2003 inclusive data sample. Thus a Neural Network prepared to be used for the 2002-2004 data sample was trained on 2004 MC. In the 2006 data sample the angular acceptance of the spectrometer is larger and the performance of the hadron calorimeters differs significantly compared to 2004. Thus for proper description of the 2006 data sample a dedicated MC was needed.

The 2006 data sample is the broadest from phase-space point of view among all considered years. This allows the NN trained on this sample to be the most general. Indeed, as shown in section 5.5, the results obtained on 2004 data sample with an NN trained on the 2006 MC are almost the same as the ones obtained with the 2004 NN. Therefore the 2006 NN was used for $\Delta G/G$ extraction for all years.

The LEPTO program was used as an event generator; the generated events were processed by COMGEANT [15] and then by CORAL [16]. When comparing data and MC, it was ensured that the same CORAL version was used for the two reconstructions. In addition the CORAL option files where kept as close to the production ones as possible in accordance with `/afs/cern.ch/compass/detector/geometry/mc`.

The following cuts were used for the inclusive sample selection:

- Selected events have a primary vertex containing a beam muon and a scattered muon.
- The scattered μ' is identified using the function `iMuPrime()` from PHAST (version 7.102). For the semi-inclusive triggers it is additionally required that there is at least one hadron track in the primary vertex (PV).
- The primary vertex is required to be contained in the target volume. The extrapolated beam track is

required to pass through the full length of both target cells. The target volume is defined by using PHAST functions: `PaAlgo::InTarget` and `PaAlgo::CrossCells` with $R < 1.3$, $Y < 1.0$ and $R < 1.3$, $Y < 1.3$ for 2004 and 2006 MC samples respectively.

- Kinematic cuts: $Q^2 > 1\,(\mathrm{GeV/c})^2$, $0.1 < y < 0.9$.

In order to obtain a good description of the data proper simulation of our apparatus was examined. For this purpose mainly the agreement for muon variables in the inclusive sample was considered. Incoming beam particles that are put into the generator were extracted from data. To properly describe the beam halo a sophisticated procedure was developed [17]. It was shown that variations of the beam profile have negligible effect on the description of the inclusive kinematic variables [18] for triggers other than the Inner Trigger. As the Inner Trigger contributes to a minority of the selected data sample it was decided to use a beam description based on 2004 for all MC samples. In order to properly simulate the background from pile-up beam particles a dedicated minimum bias MC sample was merged with the generated MC samples (The `random_rich.2004.00.outpipe.fz.*` and `random.2006.03.outpipe.fz.1` for 2004 and 2006 respectively. Both can be found at `/castor/cern.ch/user/v/valexakh/random/muplus160`).

Two important issues about the spectrometer have been found to be crucial for the proper description of the 2006 data sample. The first being the thresholds for the simulated calorimeter component of the trigger. The best values of the thresholds were selected by comparing the description of the data sample by MC for the Inclusive Middle Trigger to the one obtained for Middle Trigger. As the only difference between those two triggers is the requirement of the calorimeter signal, in Middle Trigger case for properly set thresholds both MC samples should provide identical description of the data. For the high thresholds used in the Calorimeter Trigger the Inclusive Middle Trigger sample was compared with a sample where both Inclusive Middle and Calorimeter triggers fired. Obtained [19] values of the low thresholds: $HCAL1 = 7.0$ GeV, $HCAL1 = 7.5$ GeV. High thresholds: $HCAL1 = 8.5$ GeV, $HCAL1 = 10.0$ GeV. For the 2004 MC sample the thresholds obtained previously by Vadim Alexhakin [20] were used. Low thresholds: $HCAL1 = 6.0$ GeV, $HCAL1 = 8.0$ GeV. High thresholds: $HCAL1 = 8.0$ GeV, $HCAL1 = 9.0$ GeV.

The second component crucial for proper description of the data are the efficiencies of the trigger hodoscope planes. For the 2004 MC sample they were extracted and included into COMGEANT simulation. The effect for this sample is considered to be small [21, 22]. This is not the case for the 2006 data sample where a significant region of lower efficiency was found for the Middle Trigger. For this sample it was decided to remove the problematic region by using a geometrical cut instead of extracting the efficiencies. The decision was based on the fact that the efficiencies varied considerably from period to period [19]. The function used for the rejection is presented in appendix A.

3.2 Parton Distribution Functions (PDF's), Parton Shower and MC tuning.

After correcting all issues related with the description of the spectrometer and having enough confidence that the apparatus is described to the best of our knowledge we now focus more on the physics of the simulation.

Some of these physical aspects of the simulation are described in the PDFs, the structure function F_L and in the MC tuning. These issues are discussed in the following section.

3.2.1 PDFs and Longitudinal Structure Function, F_L and Parton Shower.

The essential requirement *à priori* is that the PDF covers the same kinematic region as the data. Looking to the newest analytical developments on the PDFs MSTW 2008 is found to have a following kinematic validity region : $10^{-6} < x < 1$ and $1\,(\mathrm{GeV/c})^2 < Q^2 < 10^9\,(\mathrm{GeV/c})^2$ which is very suitable for COMPASS phase space.

Another requirement is that the parametrization of F_2 structure function and the measurement obtained by NMC experiment agree fairly well. This requirement is usually met without difficulty since most of the fits used in the extraction of PDFs already include these data.

Finally the PDF set has to be consistent with the LO approximation in our formula. Therefore in the present analysis the selected set is the MSTW2008LO [23]. As a tool to access the parametrization the PDF software library LHAPDF [24] is used.

In previous high p_T analyzes the longitudinal to transverse cross section ratio, R, was neglected. In this analysis this contribution is taken into account using the longitudinal structure function F_L. The LEPTO builtin parametrization of F_L was used (LST(11)=122). This addition mainly affects kinematics in low-x region.

In order to improve the description of the hadrons transverse momentum the *parton shower* mechanism in LEPTO has to be enabled. This poses a problem as with parton shower we simulate higher order effects while the formula for the $\Delta G/G$ is derived in LO. Impact of this will have to be taken into account for the estimates of the systematic uncertainty. On the other hand as we include part of higher order effects into the MC the argument that by restricting ourselves to LO approximation we neglect important effects is less valid.

3.2.2 MC tuning.

As this analysis relies very much on information extracted from MC simulation to have confidence in our measurement it is mandatory that the simulation describes our data as close as possible. In practice we asses this by comparing distributions of physical observables for the data and the MC. The observables is question are: x_{bj}, Q^2, y, event multiplicity, hadron momenta, hadron p_Ts and hadron z variables. The tuning of the generator parameters is an iterative procedure where by adjusting several parameters in small steps one seeks the best agreement possible.

The tuning of the MC generator parameters the 2006 sample was used. The reason behind this decision it threefold. The physics used in the simulations should be year independent. Using 2006 sample we take advantage of all the *know-how* about the spectrometer gathered since the first data acquisition. Last but not least the 2006 sample is the broadest from the phase space point of view.

Comparing data with a MC sample produced using LEPTO default tuning results in a very poor agreement for the inclusive kinematic variables and for the longitudinal momenta of the two leading hadrons. For the transverse momenta distributions the comparison is even more catastrophic (see Figs. 11 and 12).

It is interesting to note the data - MC comparison for, another variable that was often omitted, the final multiplicity is also bad, which further points that the fragmentation is not correctly described in the simulation (Fig. 13).

All these clearly shows that the LEPTO default tuning does not describe the physics of our data.

The interesting parameters governing the fragmentation in LEPTO can be divided into two sets. The first consists of JETSET parameters PARJ(41) and PARJ(42) which govern the shape of the Lund string fragmentation function [25]:

$$f(z) \propto \frac{1}{z}\big(1-z\big)^{a} exp\Big(-\frac{b\cdot m_{\perp}^{2}}{z}\Big) \tag{13}$$

The PARJ(41) and PARJ(42) are respectively a and b parameters in the fragmentation function.

The second set consists of parameters: PARJ(21), PARJ(23), PARJ(24). To simulate the transverse intrinsic momenta LEPTO uses a model based on two gaussian distributions: one for the central values and the second for the tail. Let us call them σ_1 and σ_2, respectively. σ_1, is given by PARJ(21). The amplitude of the second gaussian is a fraction of the amplitude of the first and is defined by PARJ(23).

Conveniently the two sets of JETSET parameters can be tuned separately with a minimal correlation between them. The tuning procedure is the following: first tune the fragmentation set then after getting the best agreement proceed with the tuning of the intrinsic transverse momenta.

To tune the fragmentation parameters a test was performed, in which the difference between data and MC for the kinematic variables x and y is evaluated. The MC sample used in this test is an inclusive sample without full MC chain, but acceptance corrected. The test showed that the x and y kinematic variables are largely unaffected, only for $b < 0.1\,(\mathrm{GeV})^{-2}$ there is some space for improving. Also the test shows that one obtains correct multiplicity for $a \sim b$.

Taking into account information obtained from the test and using several sets of fragmentation parameters for full chain MC simulations the set which gives the best agreement for the kinematic variables is $a = 0.025$ and $b = 0.075\,(\mathrm{GeV})^{-2}$

Concerning the tuning of the intrinsic transverse momenta component of outgoing hadrons we face and interesting problem, three parameters are used to tune essentially two physical observables, p_{T1} and p_{T2}, the transverse momenta components of the leading and sub-leading hadrons. Therefore we need to understand how these three parameters act on the p_T distributions. The PARJ(21) parameter has a direct impact on the low p_T region of the transverse momenta distributions of the hadrons. The initial slope for data - MC ratio of these distributions (within 0.4 to 0.8 $(\mathrm{GeV}/c)^2$) changes dramatically from positive to negative for as PARJ(21) increases (while keeping PARJ(23) and PARJ(24) values). A reasonably flat slope for the data - MC ratio of p_T distributions was found for PARJ(21) $= 0.34\,(\mathrm{GeV}/c)$.

A grid is made of several values of PARJ(23) and PARJ(24) between 0.01 to 0.06 and 1.6 to 3.5, respectively. After producing full chain MC simulations for all points of the grid and analyzing the data - MC agreement for p_T distributions the best values for parameters PARJ(21), PARJ(23) and PARJ(24) are 0.34 (GeV/c), 0.04

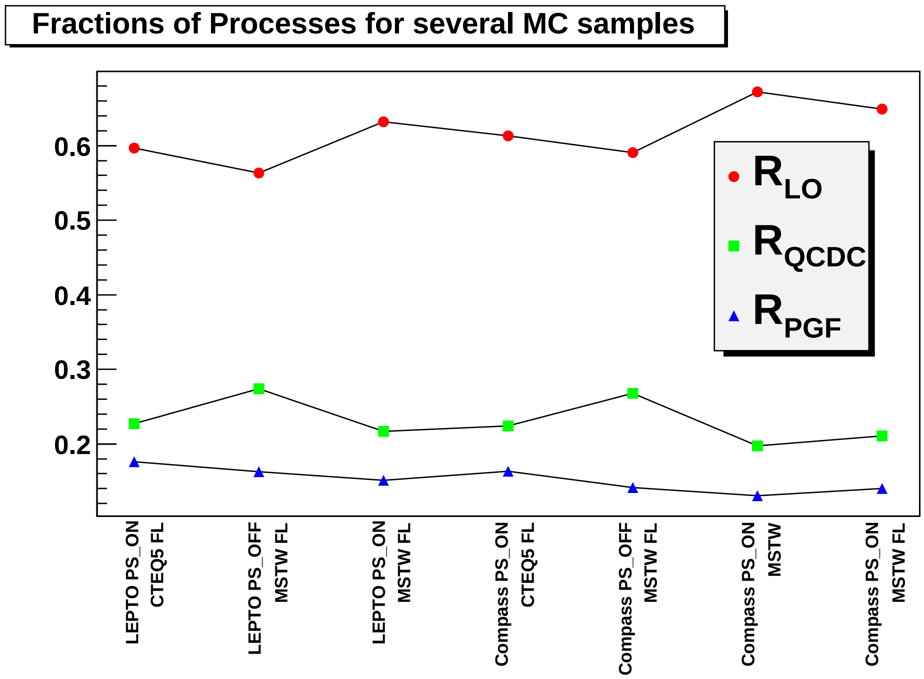

Figure 7: Fractions of processes, R, for several high p_T MC samples.

and 2.8, respectively. Table 3 summarizes the values of JETSET parameters for LEPTO default and the new COMPASS tuning, together with the old COMPASS (so-called Sonja tuning). All the details about the MC tuning can be found in ref. [26].

	PARJ 21	PARJ 23	PARJ 24	PARJ 41	PARJ 42
Default	0.36	0.01	2.0	0.300	0.580
New COMPASS	0.34	0.04	2.8	0.025	0.075
Old COMPASS	0.30	0.02	3.5	0.600	0.100

Table 3: LEPTO parameters with default, old COMPASS tuning and new COMPASS tuning values used.

3.3 Other MC samples.

Other MC samples were produced for systematic studies (sec. 5.7). Namely:

1. LEPTO DEF. tuning, parton shower ON, PDF=CTEQ5L
2. LEPTO DEF. tuning, parton shower OFF, PDF=MSTW08
3. LEPTO DEF. tuning, parton shower ON, PDF=MSTW08
4. COMPASS tuning, parton shower ON, PDF=CTEQ5L
5. COMPASS tuning, parton shower OFF, PDF=MSTW08
6. COMPASS tuning, parton shower ON, PDF=MSTW08, NO F_L
7. COMPASS tuning, parton shower ON, PDF=MSTW08

All of them were used in the systematics studies except the last one, which was used to extract the parametrization used in the analysis.

In Fig. 7 the fractions of processes, R, are compared for all MC samples. The analyzing power, a_{LL}, are shown in Fig. 8 in the same way. In Table 4 all these values are summarized.

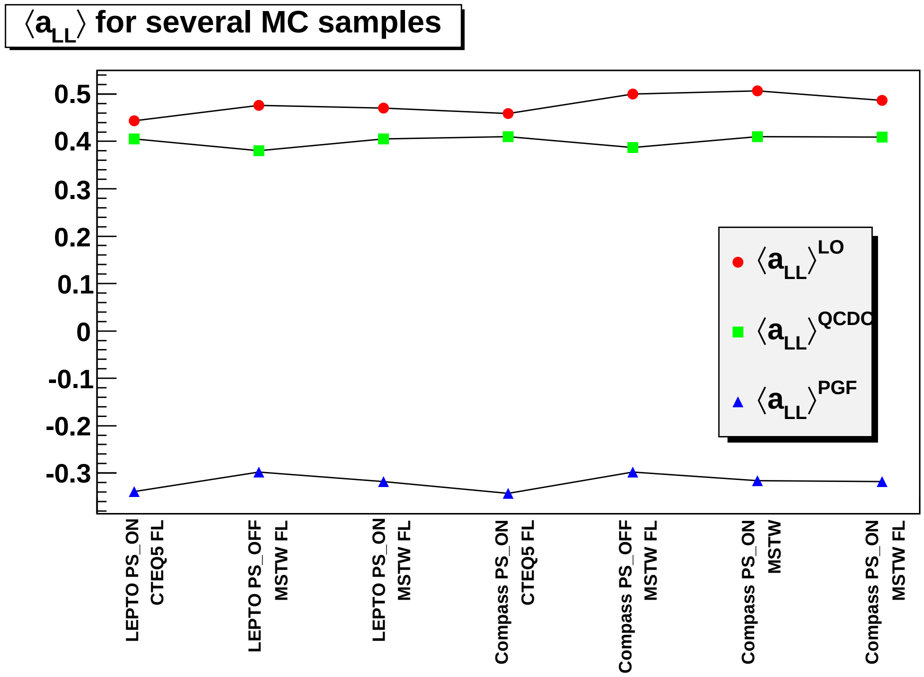

Figure 8: analyzing power *per* process, a_{LL}, for several high p_T MC samples.

	LEPTO DEF. PS ON CTEQ5L	LEPTO DEF. PS OFF MSTW08	LEPTO DEF. PS ON MSTW08	COMPASS PS ON CTEQ5L	COMPASS PS OFF MSTW08	COMPASS PS ON MSTW08 NO F_L	COMPASS PS ON MSTW08
R_{LO}	0.60	0.56	0.63	0.61	0.60	0.67	0.65
R_{QCDC}	0.23	0.27	0.22	0.22	0.27	0.20	0.21
R_{PGF}	0.18	0.16	0.15	0.16	0.14	0.13	0.14
a_{LL}^{LO}	0.44	0.48	0.47	0.46	0.50	0.51	0.49
a_{LL}^{QCDC}	0.40	0.38	0.40	0.41	0.39	0.41	0.41
a_{LL}^{PGF}	-0.34	-0.30	-0.32	-0.34	-0.30	-0.31	-0.32

Table 4: Mean values of analyzing power,a_{LL}, and processes fractions for all MC samples.

3.4 Comparison with data.

The work spent on the MC tuning paid off with a satisfactory description of experimental data both for inclusive and high p_T samples. Therefore we are confident on the quality of the MC to parametrize process fractions and a_{LL}s.

The comparison between 2006 data and MC simulation for inclusive sample is presented on Fig. 9 for the kinematic variables: x_{Bj}, Q^2 and y. For 2004 the same comparison is shown in Fig. 10. The comparison for the same kinematic variables for the 2006 high p_T sample is illustrated in Fig. 11, the hadronic variables are also shown in Fig. 12. The hadron multiplicity distributions for data and MC for the high pT sample is compared in Fig. 13. The comparison of the kinematic and hadronic variables for 2004 data and MC for the high pT sample can also be seen in Figs. 14 and 15. All distributions were normalized to number of entries.

4 Cross-check and results.

A cross-check of $\Delta G/G$ for all 2002-2006 data was performed by Konrad and Luis using independent codes, based on the data sample and the event selection, as described in section 2. All the MC data used as input are explained in section 3.

Table 5 presents a comparison between the values of $\Delta G/G$ calculated by Konrad and Luis, *per* period. Also shown are the values for 2002, 2003, 2004, 2006 and all years together. All these numbers agree up to 10^{-5}. In Figures 16, and 17 the $\Delta G/G$ cross-check for the 2002, 2003, 2004 and 2006 data is presented. The $\Delta G/G$

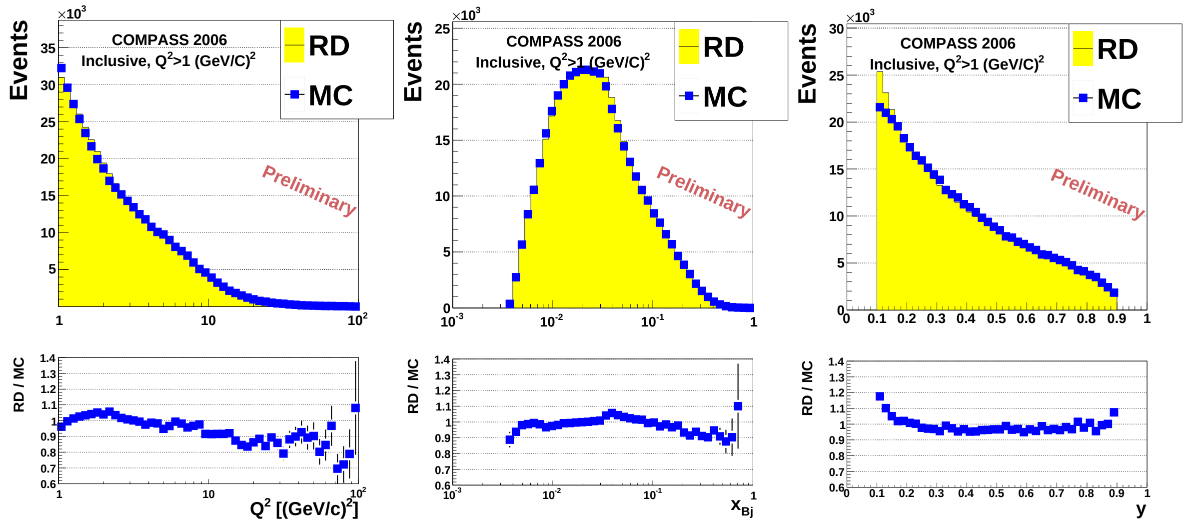

Figure 9: Kinematic distributions and data–MC comparison for 2006 inclusive sample.

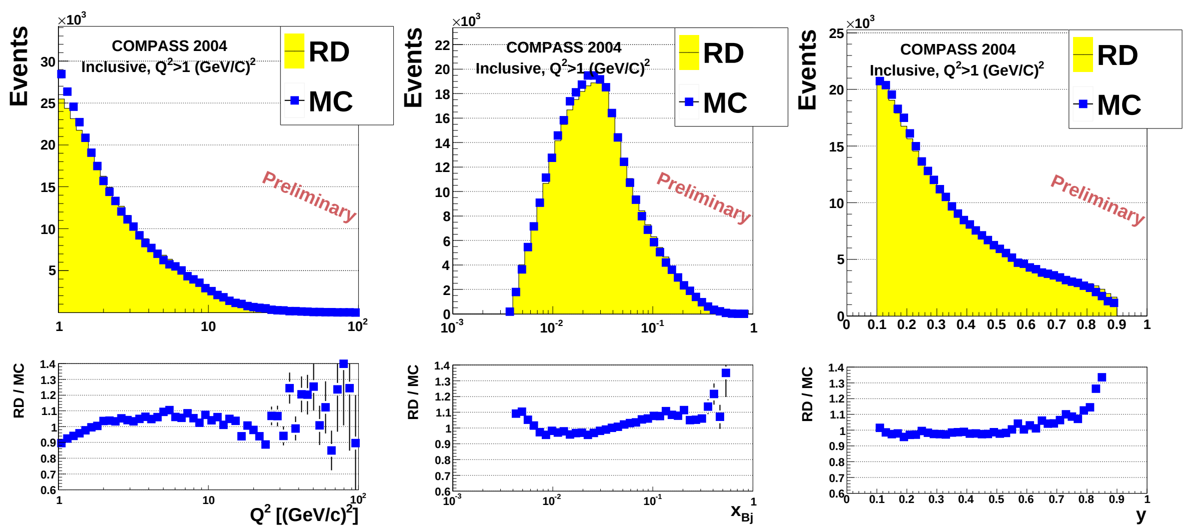

Figure 10: Kinematic distributions and data–MC comparison for 2004 inclusive sample.

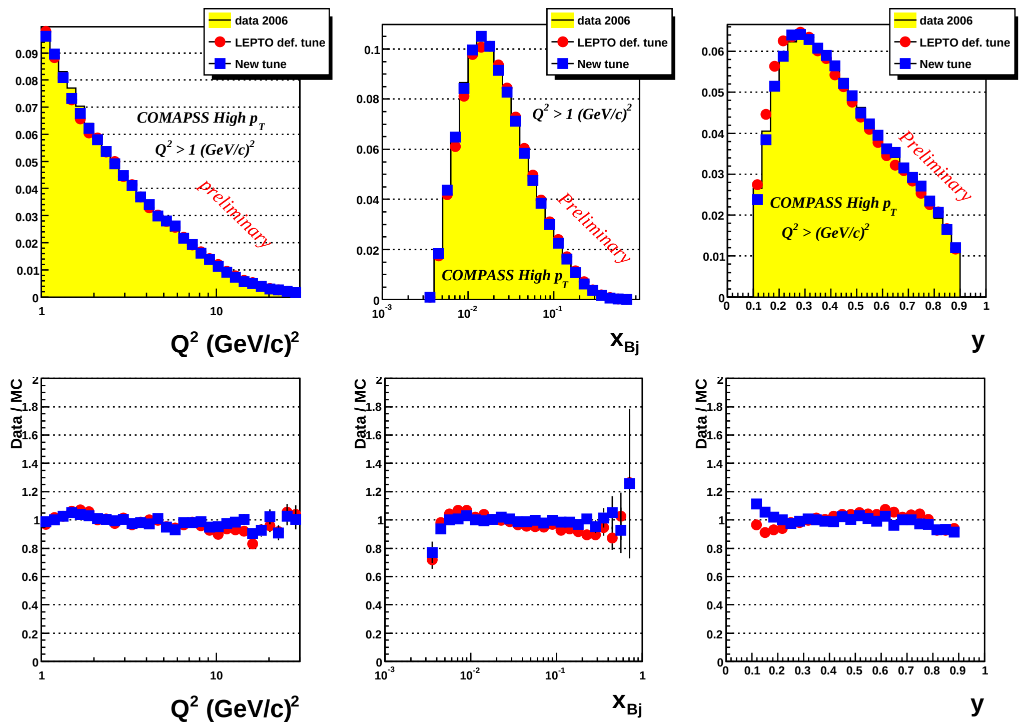

Figure 11: Kinematic distributions and data–MC comparison for 2006 high p_T sample.

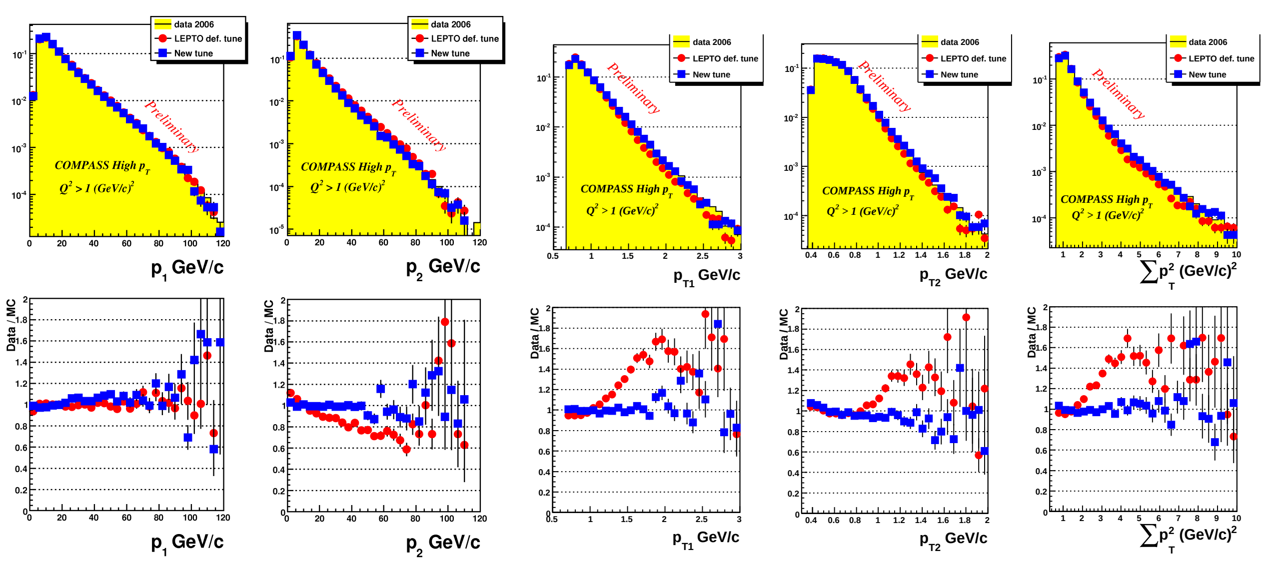

Figure 12: Hadronic distributions and data–MC comparison for 2006 high p_T sample.

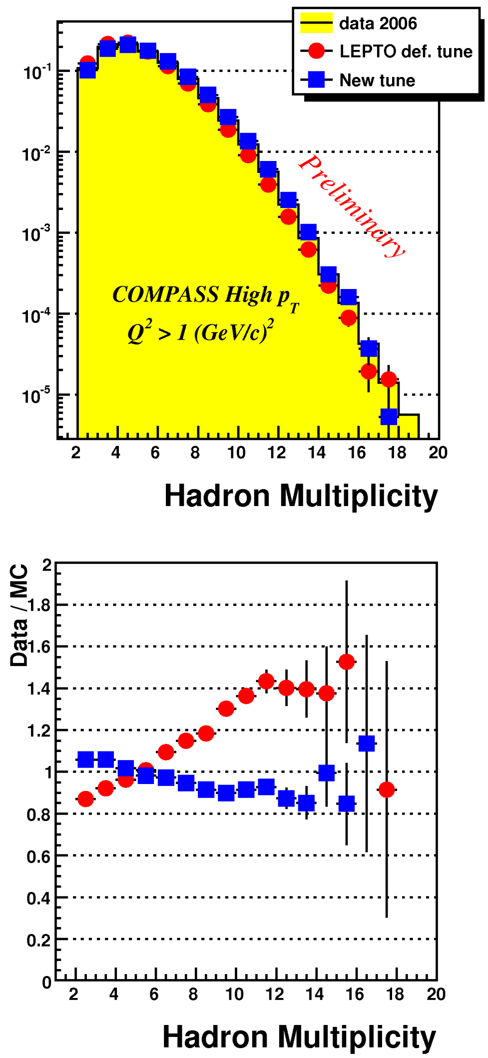

Figure 13: Hadron Multiplicity distributions and data–MC comparison for 2006 high p_T sample.

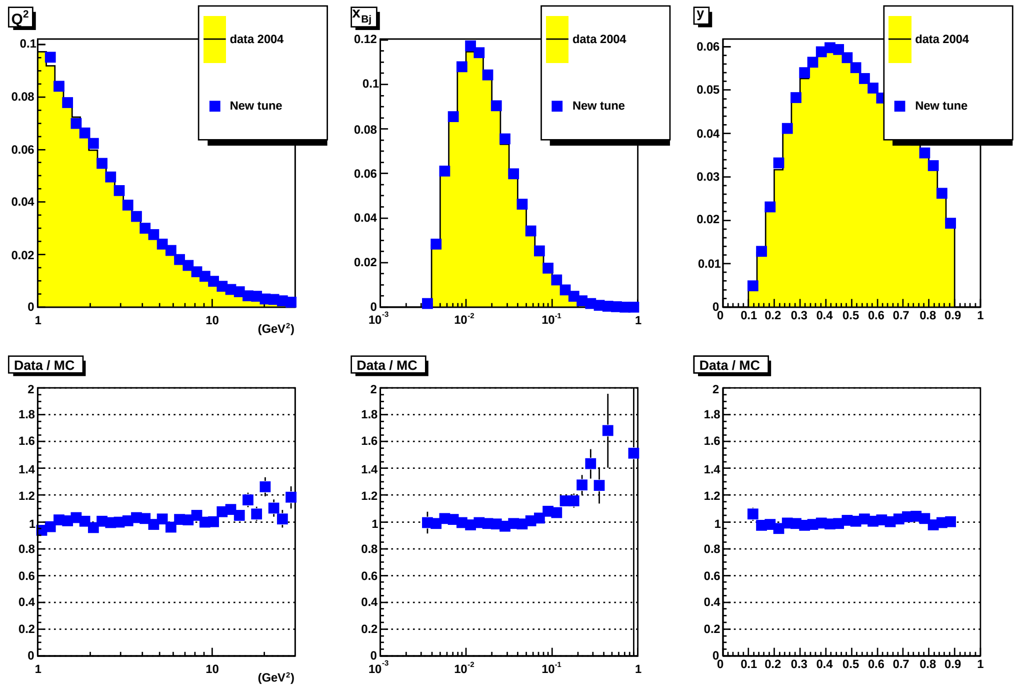

Figure 14: Kinematic distributions and data–MC comparison for 2004 high p_T sample.

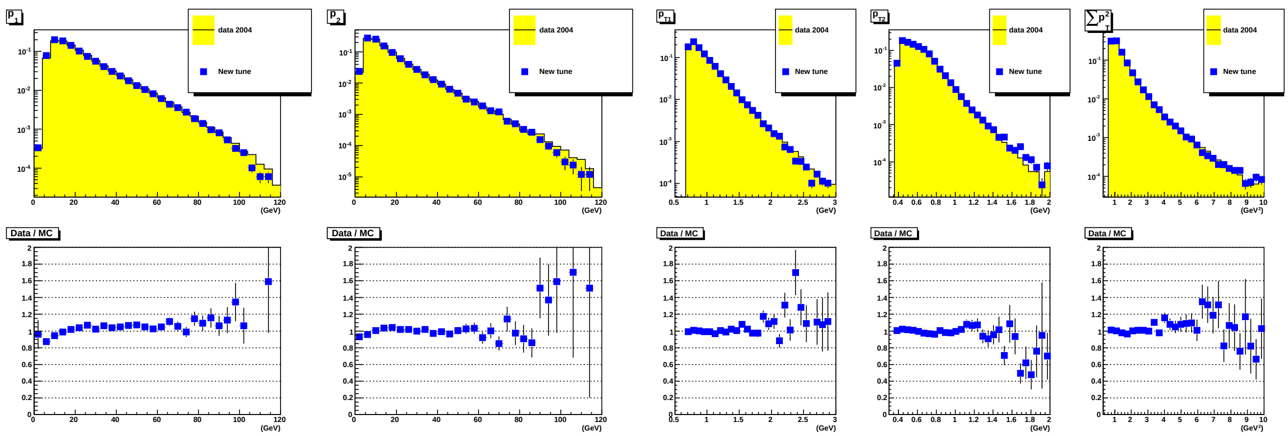

Figure 15: Hadronic distributions and data–MC comparison for 2004 high p_T sample.

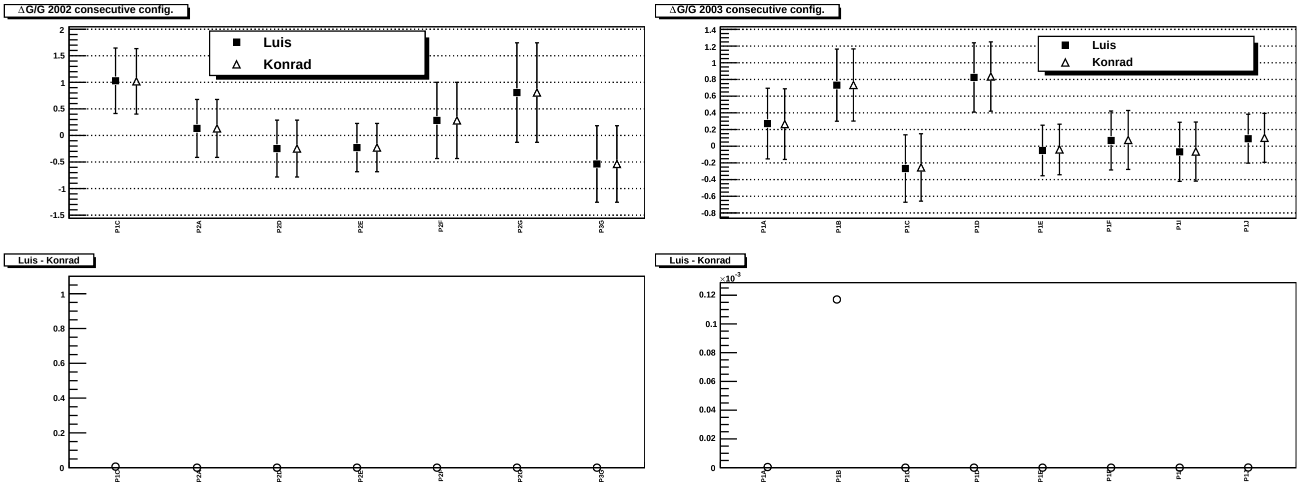

Figure 16: 2002 (left) and 2003 (right) $\Delta G/G$ cross-check and differences between two analysis.

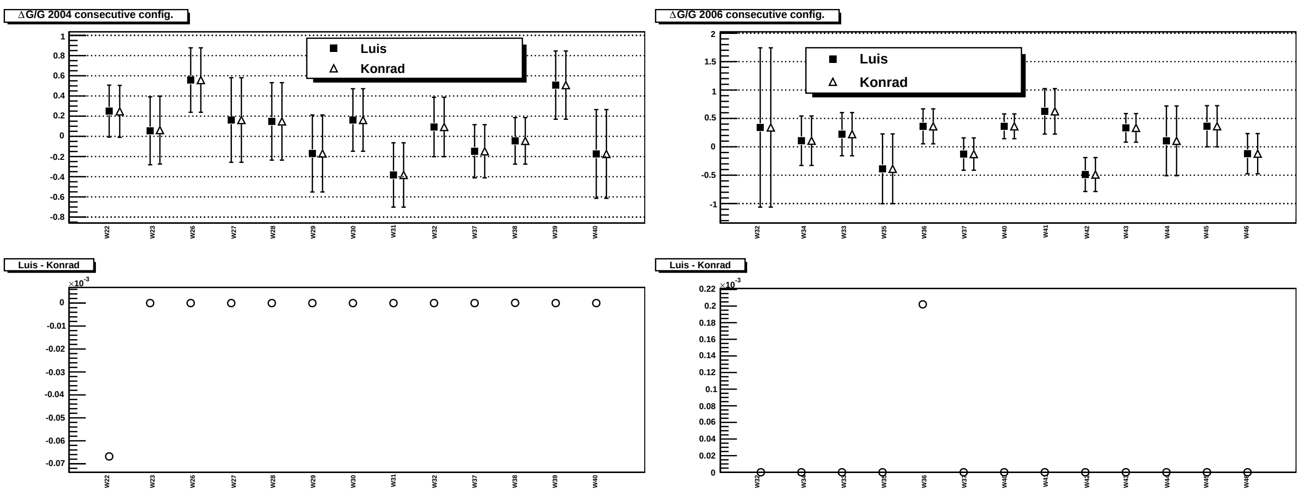

Figure 17: 2004 (left) and 2006 (right) $\Delta G/G$ cross-check and differences between two analysis.

values *per* period is shown in the upper part; in the lower part the differences (Luis - Konrad) are plotted for each period. In Figure 18 $\Delta G/G$ *per* year and for all data together is shown.

The final result (D-wave state corrected) is $\Delta G/G = 0.125 \pm 0.060 \pm 0.063$ at an averaged $x_G = 0.094$ and the x_G range covered by the measurement is $0.051 - 0.173$, with a hard scale of $\langle \mu^2 \rangle = \langle Q^2 \rangle 3.4 GeV7$. In Fig. 19 the new COMPASS high p_T measurement is presented, in which results from several experiments are also shown.

The $\Delta G/G$ was also extracted in three bins of x_G. The bin boundaries were set on x_G as returned by NN. However the interesting quantity is the x_G^{av} as shown in section1.1. Thus we obtain overlapping bins. The result in three bins is presented in Table 6 and in Fig. 20, in which results from several experiments are shown.

5 Systematic studies.

In this section the systematic studies preformed on data and MC are discussed. In many places knowledge from other analyzes is used [6], [27], [28], as well as results and ideas presented in more than 45 talks on analysis meetings given by the present and former members (Colin, Ahmed, Sonja, Roman, Sebastien, Jean–Marc) of the high-p_T group.

5.1 Samples and asymmetries used for the systematic studies.

There were a few samples used for the systematic studies. Out of them the most important are the following.

1. The "standard" high-p_T sample from which the final $\Delta G/G$ value is extracted,

	Konrad		Luis	
	# events	$\Delta G/G$	# events	$\Delta G/G$
02P1C	52374	1.002 ± 0.616	52374	1.002 ± 0.616
02P2A	82127	0.132 ± 0.545	82127	0.132 ± 0.545
02P2D	79528	-0.247 ± 0.535	79528	-0.247 ± 0.535
02P2E	110714	-0.228 ± 0.455	110714	-0.228 ± 0.455
02P2F	47087	0.283 ± 0.717	47087	0.283 ± 0.717
02P2G	27307	0.807 ± 0.937	27307	0.807 ± 0.937
02P3G	50997	-0.537 ± 0.720	50997	-0.537 ± 0.720
2002	450134	0.080 ± 0.227	450134	0.080 ± 0.227
03P1A	131079	0.259 ± 0.423	131079	0.259 ± 0.423
03P1B	113141	0.731 ± 0.432	113140	0.732 ± 0.432
03P1C	128540	-0.268 ± 0.404	128540	-0.268 ± 0.404
03P1D	128359	0.824 ± 0.415	128359	0.824 ± 0.415
03P1E	231559	-0.051 ± 0.303	231559	-0.051 ± 0.303
03P1F	182412	0.068 ± 0.353	182412	0.068 ± 0.353
03P1I	172715	-0.067 ± 0.354	172715	-0.067 ± 0.354
03P1J	275825	0.090 ± 0.293	275825	0.090 ± 0.293
2003	1363630	0.147 ± 0.128	1363629	0.147 ± 0.128
04W22	314881	0.248 ± 0.257	314880	0.247 ± 0.257
04W23	169089	0.055 ± 0.336	169089	0.055 ± 0.336
04W26	198016	0.558 ± 0.319	198016	0.558 ± 0.319
04W27	119010	0.162 ± 0.419	119010	0.162 ± 0.419
04W28	144574	0.148 ± 0.384	144574	0.148 ± 0.384
04W29	148514	-0.170 ± 0.381	148514	-0.170 ± 0.381
04W30	210282	0.162 ± 0.310	210282	0.162 ± 0.310
04W31	216447	-0.382 ± 0.319	216447	-0.382 ± 0.319
04W32	266225	0.093 ± 0.294	266225	0.093 ± 0.294
04W37	307254	-0.148 ± 0.263	307254	-0.148 ± 0.263
04W38	363844	-0.045 ± 0.231	363844	-0.045 ± 0.231
04W39	195006	0.508 ± 0.338	195006	0.508 ± 0.338
04W40	117853	-0.174 ± 0.440	117853	-0.174 ± 0.440
2004	2770995	0.076 ± 0.087	2770994	0.076 ± 0.087
06W32	12794	0.341 ± 1.402	12794	0.341 ± 1.402
06W33	104641	0.107 ± 0.435	104641	0.108 ± 0.435
06W34	155940	0.223 ± 0.380	155940	0.223 ± 0.380
06W35	60262	-0.388 ± 0.615	60262	-0.388 ± 0.615
06W36	275873	0.360 ± 0.308	275872	0.361 ± 0.308
06W37	256992	-0.128 ± 0.285	256992	-0.128 ± 0.285
06W40	466235	0.361 ± 0.218	466235	0.361 ± 0.218
06W41	147493	0.625 ± 0.400	147493	0.625 ± 0.400
06W42	316270	-0.488 ± 0.299	316270	-0.488 ± 0.299
06W43	374524	0.334 ± 0.252	374524	0.334 ± 0.252
06W44	80478	0.105 ± 0.614	80478	0.105 ± 0.614
06W45	271029	0.362 ± 0.362	271029	0.362 ± 0.362
06W46	199645	-0.121 ± 0.354	199645	-0.121 ± 0.354
2006	2722176	0.152 ± 0.095	2722175	0.152 ± 0.095
total	7306935	0.116 ± 0.056	7306932	0.116 ± 0.056

Table 5: $\Delta G/G$ values cross-check *per* period. Note that results presented in the Table **are not** corrected for D-wave state admixture in deuteron.

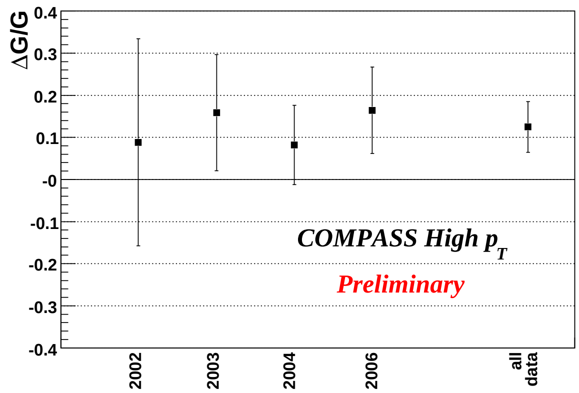

Figure 18: Final $\Delta G/G$ results for all data.

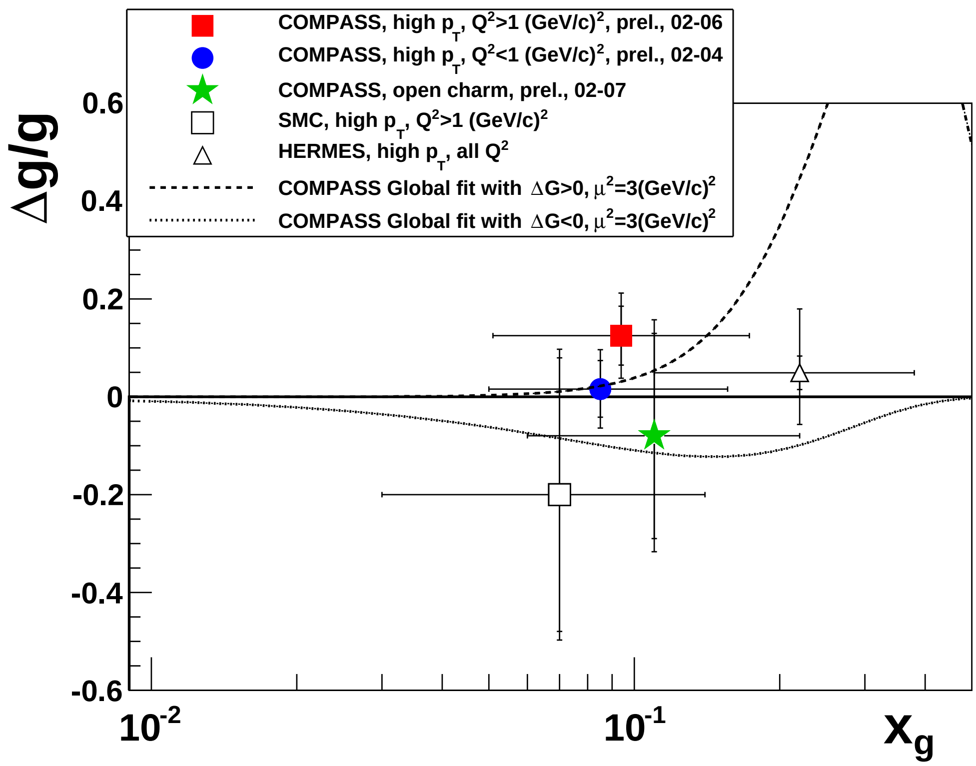

Figure 19: $\Delta G/G$ evaluated from several experiments.

	$0.041 < x_G < 0.120$	$0.059 < x_G < 0.170$	$0.107 < x_G < 0.269$
2002	-0.241 ± 0.348	0.442 ± 0.395	0.266 ± 0.975
2003	0.076 ± 0.195	0.152 ± 0.225	0.718 ± 0.509
2004	0.208 ± 0.134	-0.172 ± 0.151	0.526 ± 0.334
2006	0.203 ± 0.177	0.257 ± 0.159	-0.042 ± 0.209
Total	0.147 ± 0.091	0.079 ± 0.096	0.185 ± 0.165
$< x_G >$	$0.070^{+0.050}_{-0.029}$	$0.100^{+0.070}_{-0.041}$	$0.170^{+0.099}_{-0.063}$

Table 6: $\Delta G/G$ values in three bins of x_G. Note these results presented in the Table **are** corrected for D-wave state admixture in deuteron.

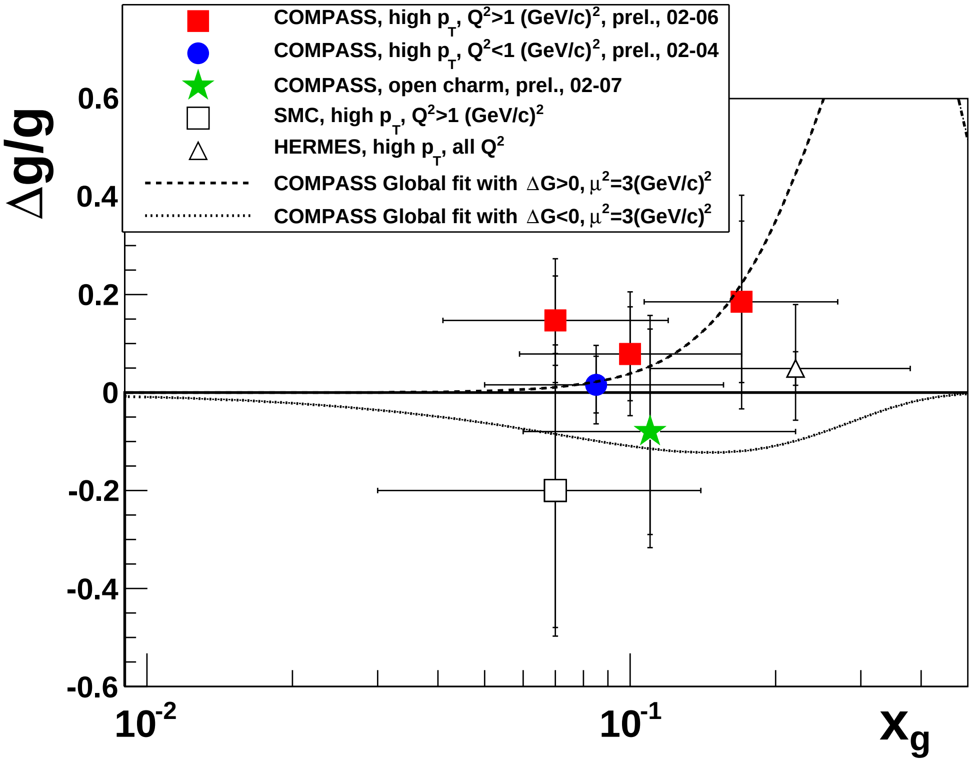

Figure 20: $\Delta G/G$ evaluated from several experiments including the new high p_T result in 3 bins.

2. The sample with looser cuts on pT and Q^2 namely $p_T 1, 2 > 0.35$ GeV and $Q^2 > 0.7$ GeV^2,

3. An all-p_T sample for which no cut is applied on the transverse momenta of hadrons.

Samples (2) and (3) have higher statistics than the (1). In order to enable relevant systematics studies of the high p_T sample, the events in sample (2) and (3) should have a similar distribution in the spectrometer as the ones of sample (1). In the high p_T, low Q^2 analysis this condition can only be met when an appropriate cut on the θ of the hadrons is applied. In the present analysis, such a cut is not crucial due to the looser cut in p_T selection. In addition, due to the moderate and high Q^2 all hadrons have some non-negligible transverse momentum with respect to the beam direction.

In the previous release only the samples (1) and (3) with $Q^2 > 1$ GeV^2 were used. However, it turned out that the sample (2), whose phase-space is much closer to our final sample's, shows larger instabilities than sample (3). Therefore the final systematic error due to false asymmetries and stability of the spectrometer is calculated using sample (2), while the sample (3) was used for additional tests.

Four asymmetries are investigated.

1. $\Delta G/G$

2. $\Delta G/G - A^{corr}/\beta$

3. $A_1^{highp_T}$

4. A_1^{2h}

$\Delta G/G - A^{corr}/\beta$ is the value for the $\Delta G/G$ obtained under the assumption that the correction of a non zero A_1^d for LP and QCDC processes can be neglected[4]. $A_1^{highp_T}$, is the A_1 asymmetry measured on the high p_T sample. In the old $\Delta G/G$ extraction, the result for $\Delta G/G$ was proportional to $A_1^{highp_T}$. Finally, A_1^{2h}, is the A_1 asymmetry measured on samples (2) and (3). As a matter of fact, this asymmetry for the sample (3) is very similar to the semi-inclusive A_1^d, since in COMPASS, there are only a few events with only one hadron in the PV. Therefore we expect a non-zero A_1^{2h} at large x.

[4]This assumption was made in the old analysis of high Q^2 data.

5.2 Validation of the sign of the asymmetries.

There is a possibility that by mistake the asymmetries are extracted with the wrong sign. There is also a possibility that the sign be extracted wrongly for one of the two microwave settings. In order to be sure that the signs are correct, the asymmetry A_1^{2h} was extracted in the high x-region and found to be positive for all years and MW setting as expected. Therefore we are confident that the signs of the extracted asymmetries are correct. One have to add that since some time the PHAST offers a function PaMetaDB::Ref().TargetSpinZproj(), which largely reduces the probability of extracting asymmetries with a wrong sign.

5.3 Global versus consecutive configuration.

In the previous release we presented results suggesting that the difference between the global and consecutive configuration (GC and CC) is not important for us. The above statement is still valid when the sample (3) is used for the systematic studies. It came as a surprise that with the sample (2) we observe larger than expected deviations between results obtained in GC and CC. In addition the RMS of the obtained A_1^{2h} in the GC is larger than one suggesting large systematic instabilities. As a consequence we decided to use consecutive configuration in which due to shorter time scale the spectrometer is more stable. Most of the discrepancies between two methods of data combining were understood like wrong alignment or *e.g.* switched off DC00 for part of 06W34. What is even more important in all considered cases it is clear that CC prevents false asymmetries. The usage of CC has its price, especially for the 2006 data. In this year where there was only one filed rotation per day and we lost about 30% of events due to the fact that many configurations do not have a partner with opposite field direction.

As it is mentioned in section 1.3, we use the second order method of asymmetry extraction. This method is known to bias the results in the case of a small number of events, as $1/\langle N\rangle \neq \langle 1/N\rangle$. With a toy MC it was seen that the bias is negligible for N> 10; as our N is at least two orders of magnitude higher we can safely neglect the effect.

5.4 False asymmetries.

Under the term false asymmetry we understand the asymmetry which should be zero or by construction, *e.g.* dividing upstream cell by half, or the difference between the same asymmetry obtained in different conditions *e.g.* difference between A_1^{2h} for day and night. Most of the false asymmetries that have been considered turn out to be consistent with 0 for all the samples. Examples of false asymmetries which have not caused the problem are:

- field reversal asymmetry for same cell divided in two halves (for one and the other cell),
- day-night,
- left-right μ'
- top-bottom μ'
- PV in the inner/outer part of the target,
- number of hadrons in the PV,
- inter-compatibility of trigger by trigger asymmetry.

On the other hand there are some interesting features of the previously reported non-zero false asymmetries, Namely the Micro Wave (MW) false asymmetry and the top-bottom hadron false asymmetry. A finite MW false asymmetry was observed in the low Q^2 high-p_t analysis and a value of $1/2(MW_+ - MW_-) = 0.008 \pm 0.001$ was reported. In the previous release of this analysis we obtained 0.007 ± 0.002, in agreement with the above. As for the top-bottom false asymmetry we have shown A_1^{2h} as a function of the ϕ angle of the leading hadron in pT. The presented distribution was not flat. The χ^2/NDF was 38/14 suggesting large false asymmetry. This false asymmetry was for the first time observed in the low Q^2, high p_T analysis. There it was also shown that this asymmetry is predicted by MC and cancels after integration over the ϕ angle if the spectrometer is top-bottom symmetric[5] [27].

[5] Which is not the case in COMPASS but the remnants of the false asymmetry are negligible w.r.t statistical errors

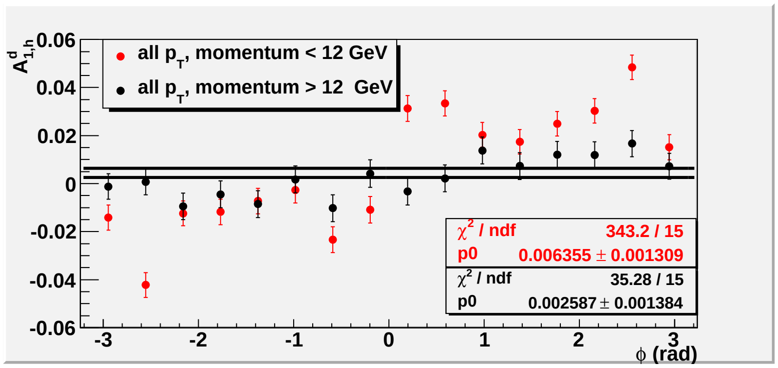

Figure 21: Top-bottom hadron false asymmetry for hadrons in different momentum ranges.

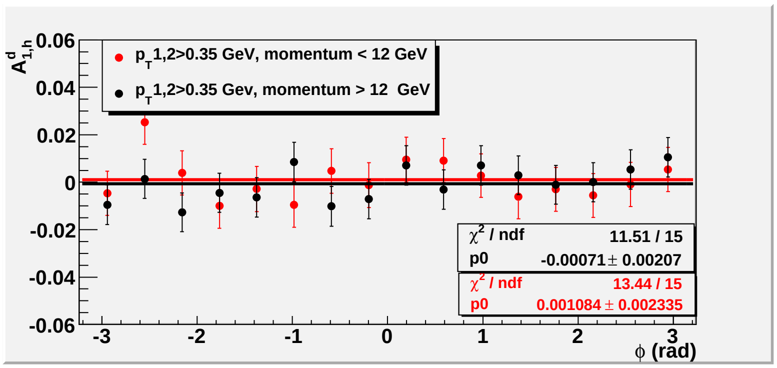

Figure 22: Top-bottom hadron false asymmetry for hadrons in different momentum ranges with p_T cut of 0.35 GeV.

In Figure 21 the A_1^{2h} as a function of the ϕ angle is shown, observe that this time both hadrons are used in the analysis. The data sample was split in two depending on the momentum of the hadrons (cut on 12 GeV) For hadrons with higher momenta the false asymmetry is largely reduced. In the next exercise, whose results are presented in Figure 22 two above samples have an additional cut: the transverse momentum of the hadron was larger than 0.35 GeV. Within the statistical error the false asymmetries are not observed. As our final sample for $\Delta G/G$ extraction has even larger hadron pT we claim that in the final sample the top-bottom hadrons false asymmetry is largely reduced and its impact is even lower than claimed in the previous release.

For the sample (2) *i.e.* the one with the cut on hadron transverse momenta, within the statistical error the MW false asymmetry is consistent with zero. $A_1^{2h} = 0.0065 \pm 0.0031$ for MW+ and $A_1^{2h} = 0.0070 \pm 0.0034$ for MW-. giving $A_{rep} = -0.0002 \pm 0.0023$. Which is a hint that also this false asymmetry may be reduced on the sample with higher pTs.

5.4.1 Internal stability of the A_1^{2h}

Let us consider the χ^2 in a form

$$\sum_{i=0}^{Nperiod} \frac{(A_{1,i}^{2h} - < A_1^{2h} >)^2}{\sigma_i^2 - \sigma^2_{<A_1^2h>}} \tag{14}$$

where $A_{1,i}^{2h}$ is the asymmetry value obtained from consecutive configuration for a given period. For the data 2002-2004 the $\chi^2/ndf = 32.8/27$. Showing consistency of the A_1^{2h}. On the other hand for the 2006 data the obtained results is $\chi^2/ndf = 26.8/12$; the probability of such occurrence is only 0.8%.

The results of A_1^{2h} between 2002-2004 and 2006 are in agreement we also do not observe any false asymmetry in 2006 data. However, the low probability value for the consistency test of 2006 data needs to be considered. Therefore we propose for the estimation of the systematic error due to the false asymmetries to use only data 2002-2004. This way the obtained limit for the false asymmetry will be larger.

Here is also worth to mention a word on the pulls and the systematic error. If we calculated pull for 2006 data the result is 1.14 ± 0.13, therefore the *upper* limit for the false asymmetries is smaller than $0.8\sigma_{stat}$. On the other hand from the exercise presented at the beginning of the section we can conclude that extraction of the pull from consecutive configuration grouped into periods leads to the conclusion that the *lower* limit of the false asymmetries is larger than $1.1\sigma_{stat}$. The two data sample results are hardly compatible with each other. One reason could be the fact that the pulls method only works properly for the so called *random* false asymmetries, and the problem observed in the data is not necessarily of this nature. A good example was given by Franco [29].

5.4.2 Estimation of the error connected with false asymmetry.

The estimate of the systematic error connected with false asymmetries is done on sample (2). The principle is to select a larger sample than the initial one and study the stability of the results. We do not want to use the pull method to claim that the limit for the false asymmetries is 0.5 of the systematic error. We say that within the statistical error the false asymmetries are not observed and precisely this is the limit for the false asymmetries.

The formula for the $\Delta G/G$ connected with statistical error is:

$$\delta\Delta G/G_{false} = \delta A_1^{2h} \cdot < \beta_{A1} >_w / < \beta_{\Delta G/G} >_w \tag{15}$$

In this analysis we have $< \beta_{\Delta G/G} >_w = < w^2 > / < w > = 0.021, < \beta_{A1} >_w = < FDP_b^2 > / < FDP_b > = 0.189$ and $\delta A_1^{2h} = 0.021$, where w is the weight of the event used for $\Delta G/G$ extraction. Finally the $\delta\Delta G/G_{false} = 0.019$.

This contribution is almost a factor of 2 larger than in the previous release. There are several reasons leading to this. The pulls are not used and in addition smaller data sample is used than previously which leads to larger δA_1^{2h}. Finally the average w for the current high p_T sample is lower due to the extended phase space. Observe that in the current release we do not add the contribution from the MW false asymmetry neither the hadron top-bottom asymmetry to the total systematic error. As it was presented these false asymmetries are largely reduced in the final sample.

5.5 Neural Network for 2004 vs 2006.

The last two years in this analysis were spent basically on understanding and improving the 2006 MC. At the end the data/MC agreement is very good as shown in the section 3. As for the 2004 MC there is some room for improvements. The biggest difference between the 2004 and 2006 data is the hadron acceptance change due to the new target magnet. Let us consider what is expected if one uses NN trained on 2006 MC for the 2004 data. The input parameters for the NN contain p_T and p_L which means there is some information about θ angle of the hadron[6] during the NN training. In addition one has to remember that the NN returns average value of the output variable in the given phase-space point of the input parameters. Taking this information altogether one would expect that the NN trained on 2006 MC and NN trained on 2004 MC should give similar results in the phase space of the latter sample.

The 2004 MC, with its current shape, was used to the NN training. Then the $\Delta G/G$ was extracted for 2002-2004 data. The same was done with the NN trained on 2006 MC and used for 2002-2004 data. The results are the following.

- 2004 MC: $\Delta G/G = 0.108 \pm 0.075$
- 2006 MC: $\Delta G/G = 0.105 \pm 0.074$

The difference between the two results is minimal for the whole data sample 2002-2006 data it would be of the order of 3% of the statistical error. For sake of simplicity and faster analysis progress we decided to use NN trained on 2006 MC for the whole data set [7].

5.6 Neural Network stability.

The first test performed was the verification that the NN output behaves as expected. The most crucial NN of the whole analysis chain is the one that computes the probabilities for any given event to be of either PGF, QCDC or LP type. Moreover, its 2-dimensional output makes it more difficult to train than simpler, 1-dimensional, NNs, like the one for a_{LL}^{PGF} estimation.

[6] note that pT is w.r.t γ^* not the beam

[7] Similar solution was done in previous analysis. There was only one MC for 2002-2004 and not 3 or as suggested by some colleagues to be fully consistent each period should have its own MC.

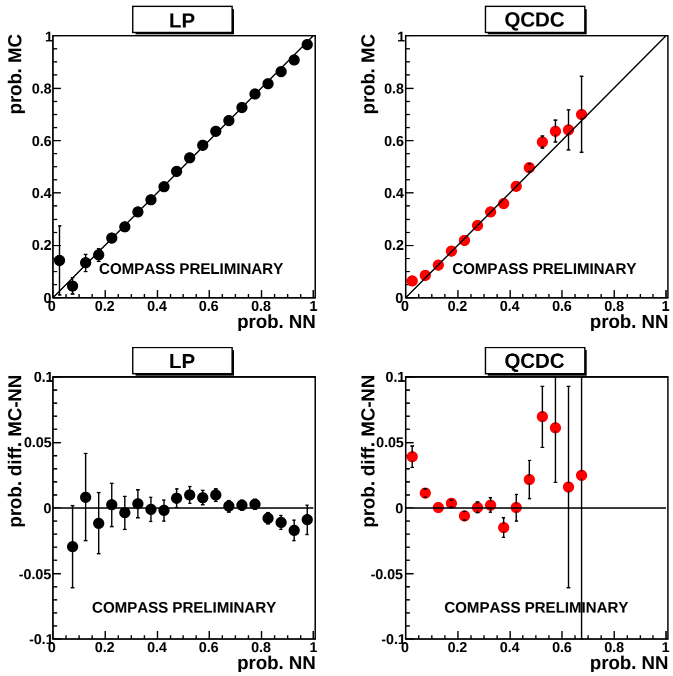

Figure 23: NN and MC comparison for R_{PGF}, R_{QCDC}, R_{LP} in bins of NN output. The lowest statistical limit for the errors is shown.

A MC data set used as testing sample, different from the learning sample used in NN training, is divided in bins of R_{PGF}, R_{QCDC} and R_{LP}. In each bin and for each process p, the fraction R_p is computed according to NN and MC truth bank. The results are presented in Figure 23. In the top part, the fractions according to MC and NN are compared and in the bottom part, the difference between NN and MC as a function of NN is presented. The results are in a reasonable agreement. Observe that the presented errors are the lowest statistical limit. They are calculated using binomial distribution, while NN does not take this into account [8].

We observe that for very low QCDC and PGF fraction some bias may be indeed observed. Such bias on the edges of the phase space are expected *e.g.* for sure we observe 0.4% events for which the Rs are negative. NN does not know about probabilistic interpretation of the results. If R_{PGF} is equal to 0 in some phase space region the output of the NN is a Gaussian centered at 0 with some RMS. Which means that the mean value is not biased but for the cost of some R_{PGF} being negative. What is important is that the observed bias has negligible effect on the final results. For example removing from the sample events with R_{PGF} and $R_{QCDC} < 0$ changes final $\Delta G/G$ by about 0.002.

In Figure 24 we present a comparison of NN and MC as a function of the sum of the p_T^2 of the two hadrons. The results from NN and MC are in agreement. Similar tests (but not so detailed) have been done for other parameters obtained from NN. In all cases, the NN output corresponds to the mean value of the given variable in MC.

In the previous release the error of $\Delta G/G_{NN}$ was estimated to be 0.006. For the current release only limited tests were done. The feeling is that the stability of the NN is worse than before. The main reason is that with the released cuts on the High pT sample the NN has to describe larger phase space *e.g.* comparing current and previous sample. The relative number of events for $\sum p_T^2 > 2.5$ GeV^2 decreased by a factor of 10. The proposed $\Delta G/G_{NN}$ is 0.010 . The result is rather educated guess than strictly obtained number. One of the problem (or luck) is that the $\Delta G/G - A^{corr}/\beta$ is very low and basically we can do almost whatever and the final results will not change much. The issue of $\Delta G/G - A^{corr}/\beta$ will be discussed more in details in the next section. One can add that values obtained from *e.g.* comparison of weight for different parametrization $\sum w_i^2/\sum w_j^2$ as suggested by J-M for open charm analysis gives systematic of the order of 0.002, which seems to be too low.

5.6.1 Alternative method of the Rs parametrization.

The usage of NN for the parametrization of Rs, a_{LL}s *etc.* is one of possible choices for this analysis. As an example in the published open charm paper [30] different method was used. The details of the method proposed

[8] simple $1/\sqrt{N}$ overestimate the NN error

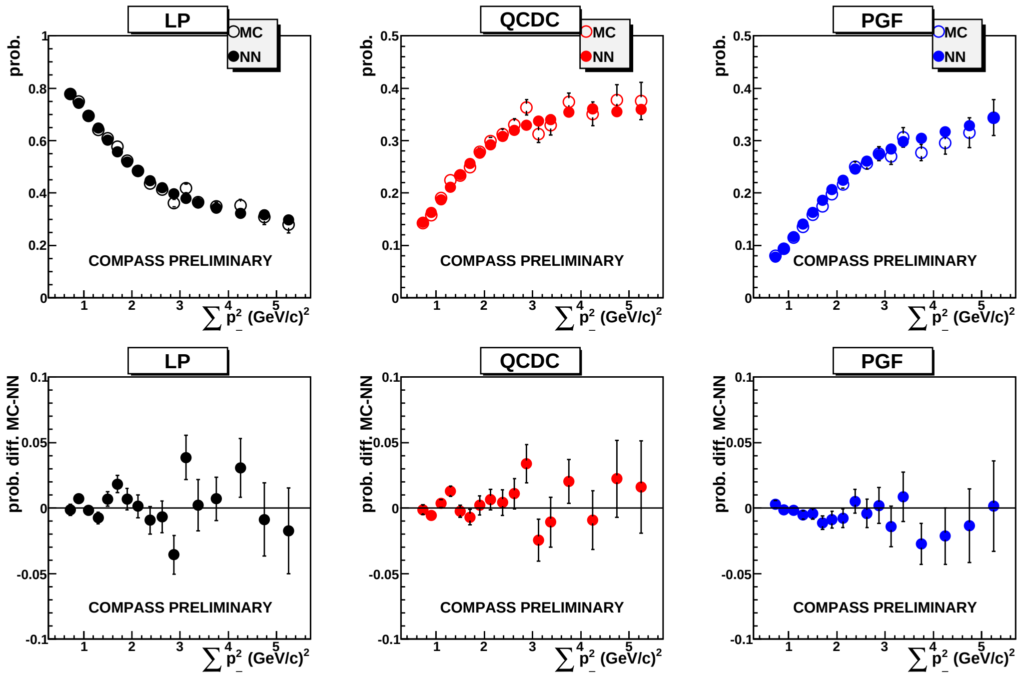

Figure 24: NN and MC comparison for R_{PGF}, R_{QCDC}, R_{LP} as a function of $\sum p_T^2$. The Lowest statistical limit for the errors is shown.

by Jean-Marc and Florian can be found in [31]. The main drawback of this method w.r.t NN is the fact that full correlation among variables cannot be taken into account. In addition, it is more sensitive to local fluctuation [9]. Contrary to NN this method cannot produce negative values of Rs but it can produce values above 1 (as NN) which leads to general observation that $R_{LP} + R_{QCDC} + R_{PGF} \neq 1$ (but very close to it). The method allows to parametrize all needed variables like xs, a_{LL}s However, for the simple test we decided to change only Rs as they have largest impact for the obtained $\Delta G/G$ results.

Observe: the exercise was performed on 2004 data with old cuts and old MC tuning done by Sonia; the results do not include $(1 - 3/2\omega)$ correction. The results are:

- standard method: $\Delta G/G = 0.1476 \pm 0.1156$,
- JM&F method: $\Delta G/G = 0.1569 \pm 0.1172$,
- the difference: 0.009 ± 0.019.

The results are in a very good agreement. One of the reason is that the dominant variable in our case is $pT1$ and correlations are not so important. Therefore, it is not surprising that the two methods give similar results.

5.7 Systematic errors due to MC.

For the following studies, as mention in sec. 3.3, seven different MCs are used.

1. COMPASS tuning, parton shower ON, PDF=MSTW08
2. COMPASS tuning, parton shower OFF, PDF=MSTW08
3. COMPASS tuning, parton shower ON, PDF=CTEQ5L
4. COMPASS tuning, parton shower ON, PDF=MSW08, NO FL [10]
5. DEFAULT tuning, parton shower ON, PDF=MSTW08

[9] With enough MC statistics, one can easily perform analysis à la J-M&F in two (or more) dimensions; in this way, a 2(+)dim correlation can be taken into account.

[10] This is to include indirectly $R(x, Q^2)$ as measured in the experiment. The R changes global cross-section while there is no information about change of subprocess fraction. On the other hand the FL from LEPTO does variate fractions of LP,QCDC and PGF.

6. DEFAULT tuning, parton shower OFF, PDF=MSTW08
7. DEFAULT tuning, parton shower ON, PDF=CTEQ5L

Employing the same strategy as in the previous release we would have in total 21 results of $\Delta G/G$: *i*) the results from MCs as they are, *ii*) the results from reweighed MC so that there is very good agreement between data and MC and finally *iii*) results where the phase space of the analysis was limited to the region where data and MC agree. After some studies, it turned out that in *ii*) tests mostly stability of the NN. The applied reweighting cannot change the Rs because it was done on the input parameters to the NN. As for *iii*) what we observe are basically statistical fluctuation due to the fact that for some MCs 40% of data were removed. Therefore in this release we propose to use only results from MC as they are.

So, we obtained 7 values for $\Delta G/G$ which are summarized in Table 7. In the first column, the version of the MC is indicated. In the second and third columns, the values and errors for $\Delta G/G$ are given respectively. Finally in the last column, the value of $\Delta G/G$ obtained neglecting the correction from A_1^d for LP and QCDC processes, a quantity that is therefore proportional to A_1^{2h} is shown. The error on $\Delta G/G - A^{corr}/\beta$ is the same as the error on $\Delta G/G$.

	$\Delta G/G$	$\delta\Delta G/G$	$\Delta G/G - A^{corr}/\beta$
COMPASS_ON_MS	0.1248	0.0601	0.0264
COMPASS_OFF_MS	0.1266	0.0578	0.0194
COMPASS_ON_CQ	0.0930	0.0521	0.0342
COMPASS_ON_MS_NOFL	0.1349	0.0716	0.0405
DEFAULT_ON_MS	0.1239	0.0480	0.0078
DEFAULT_OFF_MS	0.1578	0.0451	0.0139
DEFAULT_ON_CQ	0.1114	0.0410	0.0190

Table 7: Results for $\Delta G/G$ using various MCs. See text for details.

All the results presented in the table 7 are very close to each other. The RMS of the obtained $\Delta G/G$ is 0.020 and 0.011 for $\Delta G/G$ and $\Delta G/G - A^{corr}/\beta$ respectively. One can even notice that the last but one result is more than three standard deviation from zero. However, as one can observe in the last column of the table, the measured asymmetry is in perfect agreement with zero. The average 2 sigma effect is generated by the correction from QCDC process which are quite large since $A_1(x_{Bj} = 0.14) \approx 0.10$ is far from zero.[11] Our $\Delta G/G$ must compensate the above contribution so that the final observed asymmetry is zero. The results for parton shower ON/OFF are very similar. To be self-consistent the analysis should be done for parton shower OFF; unfortunately we were not able to achieve satisfactory the description of the data by MC using PS_OFF case. There is one worrying point namely the error in the extreme case differs by a factor 1.75 (0.0716/0.0410). We want to take this fact in to account in the systematic error.

In the previous release we decided to use the following formula for estimate of the systematic error connected to MC

$$\delta\Delta G/G_{MC} = \frac{RMS(\Delta G/G - A^{corr}/\beta)}{\Delta G/G - A^{corr}/\beta} \cdot (\Delta G/G - A^{corr}/\beta + \delta(\Delta G/G - A^{corr}/\beta)) = 0.036 \qquad (16)$$

Here, we use the results from the COMPASS_ON_MS case as a input parameters. This result looks reasonable and it is very close to the value in the previous release (0.040). However, the problem is the method works perfectly in the case of non-weighted methods of the asymmetry extraction. In the weighted case they are second order effect which starts to dominate in case of low values of $\Delta G/G - A^{corr}/\beta$. As an example, let us consider the case when DEFAULT_ON_MS is used for the systematic error estimation. The error is then 0.079, more than a factor 2 larger than before. It is true that the error is overestimated in this case so we are on the safe side. However we have a feeling that it is too random, especially if the final goal is the estimation of the systematic for each x_G bins separately.

Therefore we would like to propose other method of the systematic calculation which takes into account large difference between the error for various MCs. The method uses ratio of the error bars between the extreme cases (*i.e.* 1.75), for safety we again make an assumption that the measured $\Delta G/G - A^{corr}/\beta$ is defined by

$$\Delta G/G - A^{corr}/\beta = max(\delta\Delta G/G, |\Delta G/G - A^{corr}/\beta|) = 0.060 \qquad (17)$$

The systematic error connected to MC would be then

[11] there are some proportionality factors involved but for by chance they are very close to one for the current release

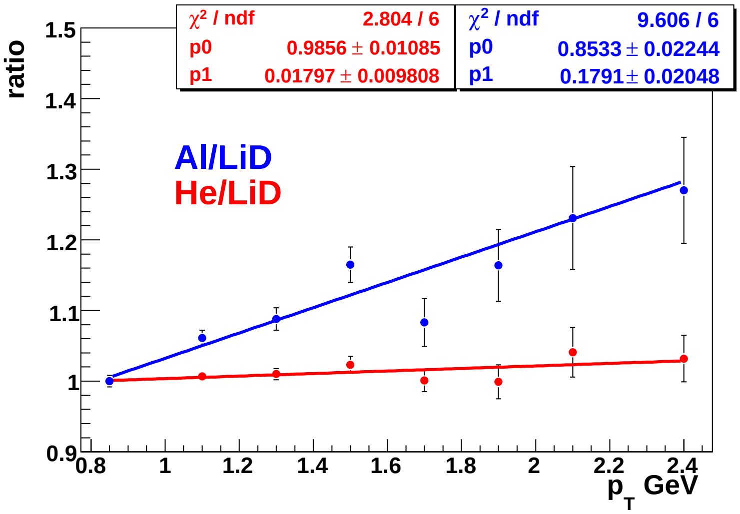

Figure 25: The ratio of the observed number of events for different nuclei in bins the hadron pT.

- $0.06(1/1.75 - 1) = -0.026$,
- $0.06(1.75 - 1) = +0.045$.

The error is asymmetric we can use is it or not [12]. Taking the maximum of the difference between the error bars is quite dramatic usually one would take 1/2 of it but the error in such a case is rater low. The benefit form the method is that it is more stable that the previously used and is easier to describe *e.g.* in a paper. Most of other methods will give much smaller errors. One can of course use "brute force" solution and change R_{PGF} by a factor 2 up or down. The results are: 0.306 ± 0.132 $(1/2R_{PGF})$ and 0.0435 ± 0.0272 $(2R_{PGF})$.

5.7.1 The $cut-off$ parameters.

In the analysis meeting Feb 2009, Aram presented results which shows that the so called $cut-off$ parameters[13] may influence our $\Delta G/G$ results. After discussion the High pT group decided that instead of changing the $cut-off$ parameters we will use two different $cut-off$ schemes with their default values of the parameters. This systematic effect is already included in the presented results for $\delta\Delta G/G_{MC}$. The decision was not unanimous there was one vote against this proposition.

5.8 δP_b, δP_t, δf.

The relative error of δP_b, δP_t is taken as 5% and 2% for $\delta f/f$. It is assumed that the systematic error of $\delta(\Delta G/G)_{fP_bP_t}$ is proportional to the errors given above. The total contribution to the systematic error is $\delta(\Delta G/G_{fP_bP_t}) = 0.004$. The value is very small even if again we have used a safety margin to take into account that the measured $\Delta G/G - A^{corr}/\beta$ is close to zero.

The error of the dilution factor is quite small. The HERMES results [32] suggest that for larger nuclei the dilution factor depends upon transverse momentum of the hadron. Some tests were done and the results were presented in [33]. The analysis is summarized in the Figure 25. It is shown the ratio of the p_T distribution for the hadrons produced in He and Al environment to the hadrons produced in the target LiD. In the case of this analysis, we must pay attention to the He contribution, but within statistical errors the ratio He/LiD is flat. Therefore, we assume that f(pT) has rather week dependence for our LiD target. Of course, one could increase the $\delta f/f$ to be on the safe side. On the other hand we do observe a clear effect for Al/LiD. Taking into account the size of the corresponding nucleus one can expect that in the case of NH_3 target the observed effect should be even larger. Therefore without a dedicated measurements of this effect it may be difficult to incorporate 2007 and eventually 2011 proton data to the current analysis.

[12] In the section concerning systematic error connected to the simplification of the formula for $\Delta G/G$ extraction there will be some comment concerning the above choice.

[13] These are unphysical parameters used to remove divergences from integrals

5.9 Systematic error related to the A_1^d parametrization.

Four parametrization of A_1^d are used to estimate the associated systematics. They are:

- v1: world data fit, all Q^2, [34]
- v2: world data fit $Q^2 > 1$ GeV^2
- v3: fit to COMPASS data only $Q^2 > 1$ GeV^2
- v4: simple fit $A_1^d = x^{1.24}$

The analysis was done for the *global* configuration The obtained results are presented in Table 8. The RMS of these results is used as an estimate of the uncertainty connected with the A_1^d parametrization. The estimated error is $\delta(\Delta G/G)_{A1} = 0.015$. For the final $\Delta G/G$ result, the published fit of A_1^d ($v1$) is used. The observed trend in the results is the same as in the previous release. Note that, with the released kinematic cuts, the average weight of the events is lower than in the previous release. This leads to a bigger sensitivity to the uncertainty of A_1^d parametrization (previously this contribution was 0.008).

version	$\Delta G/G$
v1	0.131 ± 0.056
v2	0.134 ± 0.056
v3	0.162 ± 0.056
v4	0.155 ± 0.056

Table 8: Results for $\Delta G/G$ using various A_1^d parametrization.

5.9.1 Extraction of $\Delta G/G$ using PDF.

Instead of A_1^d parametrization one can use LO PDF obtained by various groups. Note that in case of LO PDF it is assumed that all interactions come from LP. Therefore the weight in the analysis has to be modified, it does not include the correction where Rs_{incl} appears. This in turn leads to decrease the obtained error of $\Delta G/G$ [14]. Of course, this is too large simplification. Therefore the results presented below are just for information only. They are not used in any systematic calculations. The results were obtained for 2002-2004 with previously used cuts, tuning and old mDST, *i.e.*, the results called “standard method” is the previously released $\Delta G/G$ value (with one more numerical digit). As one can see in the Table 9 the various PDF give results similar with each other and also with the previously released $\Delta G/G$ value.

PDF	$\Delta G/G$
standard method	0.083 ± 0.101
COMPASS ΔG+	0.074 ± 0.083
COMPASS ΔG-	0.073 ± 0.083
DNS	0.083 ± 0.083
LSS	0.058 ± 0.083
ACC	0.081 ± 0.083
GRSV	0.086 ± 0.083
DSSV	0.093 ± 0.083

Table 9: Results for $\Delta G/G$ using various LO PDF parametrization. Note that improvement in the error bar is a results of the formula over-simplification! The exercise was performed on old sample and old MC tuning!

5.10 Non-pion contamination.

To obtain the formula for $\Delta G/G$ *c.f.* equation(1) it is assumed that only pions are produced in the final state, so that the fragmentation functions cancel out, and $\Delta G/G$ can be factorized. In the data sample, there are about 30% of events where a non-pion particle is selected. For the tests, such events are removed in a two ways (two samples are tested) using RICH in formation: *i*) positive pion identification, *ii*) kaon and proton identification.

[14] the looser cuts the “gain” is larger.

The obtained results in both cases are in agreement with $\Delta G/G$ from the whole sample. The correlation factor between the samples was taken into account. Note however, that a difference by 30% in the number of events allows a statistical fluctuation on a sigma level larger than 0.5. Therefore, the described test is a weak one. This test was done for the previous release. After the release some additional test was done. The additional MC samples was produced, which contained only pions, and used for NN training. The analysis was repeated on the full data set i.e. without PID identification. The final results are in agreement within statistical error.

- Standard: $\Delta G/G = 0.1476 \pm 0.1156$,
- Pion only: $\Delta G/G = 0.1399 \pm 0.1148$,
- the difference: 0.008 ± 0.014,

where the error is the lowest limit taken from $\sqrt{0.1156^2 - 0.1148^2}$. These results were reported on Aug 2008 analysis meeting. This test was done on 2004 data only, with old cuts and with old tuning, furthermore $(1-3/2\omega)$ correction is not included.

5.11 Radiative corrections.

Radiative corrections are properly treated for data in dilution factor calculation. However inclusion of the longitudinal structure function F_L to the cross section parametrization used by the MC generator requires for a proper treatment of radiative corrections for the inclusive MC sample. The two effects cancel out to a high degree and cannot be applied separately as this would lead to large discrepancy with the real data. Radiative corrections were included into the inclusive MC via application of radiative weights from tables used in dilution factor calculations, The tables were prepared for both inclusive and semi-inclusive events and are parametrized in x_Bj and y variables. The MC events were reweighted with RC both for comparison with real data and for training of Neural Networks.

To estimate the upper limit of expected effect on the high p_T-sample the tables for semi-inclusive events were used. The radiative corrections for high p_T events are expected to be smaller then in the semi-inclusive case as the phase space available for the photon emission is largely reduced. The effect of reweighting high p_T events with radiative corrections weight tables was found to be negligible for inclusive variables as well as for average values of a_{LL}s and processes fractions 10. The impact on the hadronic variables is hard to estimate as tables cannot account for change in kinematics of virtual gamma with respect to which the p_T is calculated. Unfortunately a working implementation of RADGEN in LEPTO is currently not available.

	R^{PGF}	R^{LP}	R^{QCDC}	$< a_{LL}^{PGF} >$	$< a_{LL}^{LP} >$	$< a_{LL}^{QCDC} >$
Inclusive	0.07	0.83	0.10	-0.27	0.40	0.38
Inclusive + RC	0.07	0.83	0.10	-0.26	0.39	0.37
Semi-inclusive	0.06	0.85	0.09	-0.27	0.38	0.35
Semi-inclusive + RC	0.06	0.85	0.09	-0.27	0.38	0.35

Table 10: The effect of the radiative corrections in inclusive and semi-inclusive MC samples: fractions of the processes and a_{LL}'s.

5.12 Resolved photon contribution.

Apart from the three LO processes also *resolved photon* processes could contribute to the cross-section. A contribution of such processes was found to be significant, of the order of 50%, in the low Q^2 *high* p_T analysis [27]. The RAPGAP [35] generator was used to estimate the contribution of the resolved photon processes to our sample. In RAPGAP the three LO processes and the resolved photon ones have to be generated separately and then weighted with the obtained cross-sections. Unfortunately the parton distribution functions of the photon are poorly known which leads to a variation of obtained cross-section by few orders of magnitude depending on the selection of PDFs. Thus to estimate the resolved photon contribution a fitting procedure was developed.

The kinematic distributions of events originating from the resolved photon differ significantly from distributions of LEPTO events (Fig. 26) This allowed to estimate the fraction of resolved photon events in the *high* p_T sample. A sum of LEPTO and resolved photon distributions was fitted to the experimental data with one free parameter f, the fraction of LO events:

$$S = f \cdot LEPTO + (1 - f) \cdot Resolved\,photon. \tag{18}$$

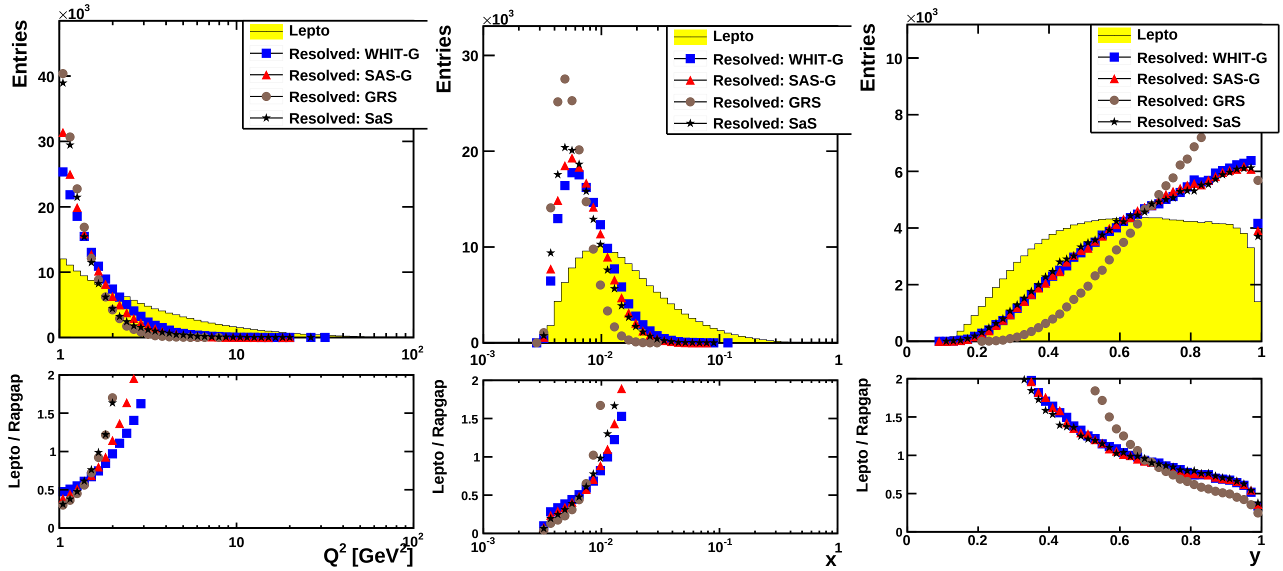

Figure 26: Comparison of kinematic distributions of events generated by the LEPTO with distributions of events originating from resolved photon processes obtained form the RAPGAP. Different points correspond to several selections of the photon PDFs.

The fits were performed in a 2D space (Q^2, y) for nine different photon PDFs [15] and for three different μ^2 scale selections. The three considered scales were the following: $\mu^2 = 4 \cdot m^2 + p_T^2$, $\mu^2 = Q^2 + p_T^2$ and $\mu^2 = \hat{s}$.

To account for the spectrometer acceptance the events generated by LEPTO were processed by a full MC simulation. As we lack interface between RAPGAP and COMGEANT the resolved-photon distributions were weighted with 2D $\left(Q^2, y\right)$ acceptance obtained from the full LEPTO simulation. The fits were performed for each trigger independently.

Selected fits are presented in Fig. 27. The biggest resolved photon contribution is observed for the IT sample which is consistent with the results of the low Q^2 *high* p_T analysis [27], where this trigger was dominant. For $Q^2 > 1\,\mathrm{GeV}^2$, the IT corresponds to 0.4% of the data sample and obtained resolved-photon contribution for the whole sample is well below 1%.

The values of fragmentation parameters were tuned to obtain a better description of the experimental data. When doing this we might compensate for not simulated resolved photon events by an artificial change of fragmentation parameters. To test this another fit was performed using distributions obtained from simulations with the default setting of fragmentation parameters. The obtained fraction is $\sim 5\%$, however with obtained quality of the fits it is not possible to judge if such MC simulation would describe data better than the one used for extraction of the final result.

In the low Q^2 analysis, where resolved photon events correspond to a half of the sample, the systematic effect due to the lack of knowledge about polarized photon PDFs leads to about 10% relative error on $\Delta G/G$. In our case we can safely neglect the resolved photon contribution, both to the final result and to the systematic error.

5.13 Simplification of the formula for $\Delta G/G$ extraction.

The impact of the x'_C factor in the eq.(10) was estimated in two tests. In the first one, x'_C was assumed to be proportional to x_C, $x'_C = 1.6 \cdot x_C$. In the second x'_C was approximated by using x_C instead of x_{Bj} as an input parameter for NN which estimates x_C. Therefore $x_C(x_C(x_{Bj}))$ was calculated. The resulting change of $\Delta G/G$ was 0.024 and 0.035 respectively. For the systematic error estimate we assumed that $\delta(\Delta G/G_{formula})$=0.035. In the previous release, the error value was only 0.012. Therefore, this contribution was studied in more details. The correction is in the form of $const \cdot Asy(x'_c)/w$. The c has changed only by 5% and so, it cannot be the reason of this discrepancy. The $< w >$ changed by almost 35%. But, taking into account the correlation between c and w, it turned out that the change from the point of view of the weighted method for the asymmetry extraction is: $< c \cdot w > / < w^2 >$ is 1.75. And the last, whereas in the previous release the $\log(x_C)$ was calculated, now

[15] GRS (1), SASGAM (2): the numbers in brackets correspond to the values of the 'INGA' option of the RAPGAP generator [35]. DO-G (311), LAC-G (331), GS-G (341), GRV-G (351), ACFGP-G (361), WHIT-G (381), SaS-G (391): the numbers in brackets correspond to the ID number of a PDF in the LHAPDF library [24].

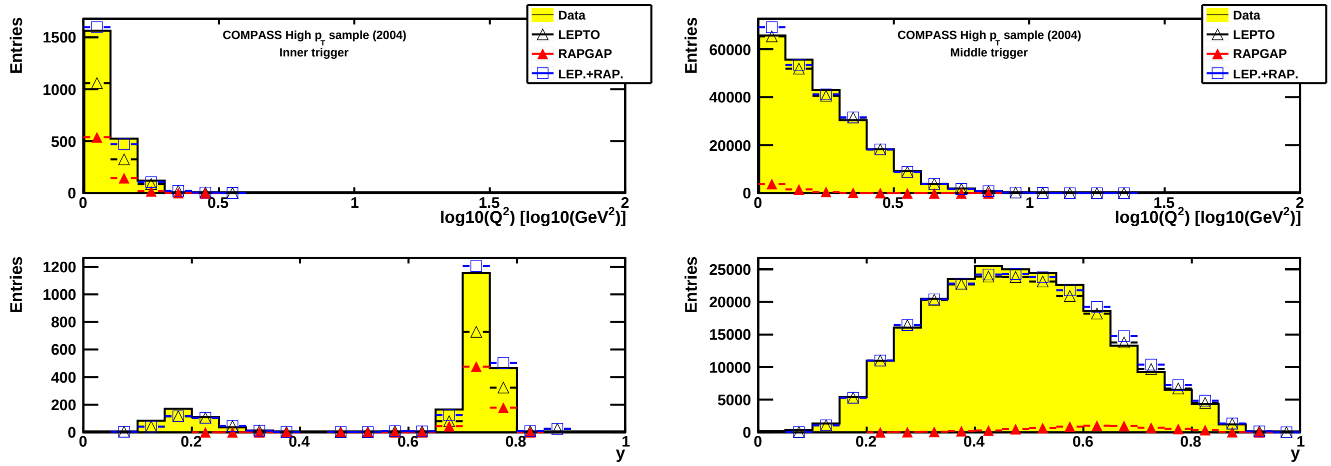

(a) (b)

Figure 27: Q^2 and y distributions for the LEPTO LO and the RAPGAP resolved photon simulations compared to the experimental data. The RAPGAP simulations are done with the photon PDFs of Ref. [36] and with scale $\mu^2 = m^2 + p_T^2$. The MC distributions are normalized to the fraction obtained from 2D fit to data (*cf.* text for details). The results are presented for two samples: a) Inner Trigger and b) Middle Trigger. The green circles represent the sum of LEPTO and RAPGAP distributions.

x_C is calculate directly. In addition, $A_1(x_C)$ is correlated with the weight. Finally, taking into account all these factors, the correction is larger by a factor 2.8 than before, i.e., very close to what it is observed on the data.

Please note that this correction can be **only** negative. In fact if one combines asymmetric error from MC systematic one obtains as a final errors -0.044 and +0.045. Taking this opportunity one can reduce final systematic error by about 20%. We do not propose this solution. In addition in the final error estimation we assume that the $\delta(\Delta G/G_{formula})$ can have both signs to avoid having asymmetric errors ***to be discussed***.

5.14 Miscellaneous.

5.14.1 Weight and systematic error.

Let us do a following academic exercise. We perform an asymmetry measurement as in COMPASS. Unfortunately the data after the field reversal have different acceptance than before, so that $acc_u acc'_d/acc_d acc'_u \neq 1$. This obviously leads to a bias of extracted asymmetry. Now let us assume that we use weighted method of the asymmetry extraction and that the correlation between acceptance change and the weight is **zero** [16]. In such a situation, it can be shown that the asymmetry will be extracted without a bias. If one plots the asymmetry as a function of $1/w$ and fits a straight line $a(1/w) + b$, then the b parameter is the asymmetry value extracted without a bias [17]. This exercise also leads to two more general statements i) in typical cases the lower the weight is the possible bias of the asymmetry is larger and ii) in the case where the weight changes the sign (like in High pT analysis or open charm), the resulting asymmetry is less sensitive to false asymmetry than A_1^d, where the weight stays always positive.

Therefore, it is not surprising, that making a cut on the weight, we can reduce the systematic error. In our case, we could reduce contributions to the systematic error coming from $\Delta G/G_{false}$, $\Delta G/G_{A_1}$, $\Delta G/G_{formula}$. As an example we show a systematic error reduction for the false asymmetries contribution. The results are presented in Table 11. In the first column, the used cut is shown; in the second, the obtained error of $\Delta G/G_{false}$ is quoted, and in the third column, the percentage of events which survive the cut is displayed and finally, in the last column, the increase factor of the statistical error for $\Delta G/G$ with respect to the is shown. The systematic error can be decreased by about 20%. It is also worth to mention that one can reduce the data sample by a factor 4 and increase the error of $\Delta G/G$ by only 4%. Similar gain can be achieved for $\Delta G/G_{A_1}$ and $\Delta G/G_{formula}$. Although the reduction of the systematic is possible by using a cut on the weight, the high-pT group does not propose this solution.

[16] obviously not always the case in the real experiment

[17] obviously in the most cases the error of this asymmetry is larger than in the case where weighted mean is used

cut	$\Delta G/G_{false}$	events %	$\delta\Delta G/G$ ratio
$w^2 > 0$	0.025	100	1.000
$w^2 > 1E-5$	0.024	58	1.003
$w^2 > 3E-5$	0.022	44	1.010
$w^2 > 1E-4$	0.021	27	1.038

Table 11: Impact of the cuts on the weight. See text for details.

5.14.2 Comparison between results obtained in "old" and "new" kinematic regions.

In the previous release we use the cuts the following cut on the transverse momentum of the hadrons and invariant mass of the hadron system. $pT1,2 > 0.7$ GeV and $M_{inv} > 1.5$ GeV. In the current release the $pT2$ cut was lower to 0.4 GeV and the cut on the invariant mass was removed. The $\Delta G/G$ values in the old domain and in the region which was added are the following:

- $\Delta G/G_{old\_region} = 0.1230 \pm 0.0843$,
- $\Delta G/G_{new\_region} = 0.1372 \pm 0.0742$.

The test was done for global configuration. The results are in a very good agreement. Note that the application of less restrictive cuts is possible due to the use of NN method in the analysis. This implies the full application of the weighting procedure. In the previous method, the release of the cuts would increase the statistical error. Using old method with previously optimized cuts $p_T1,2 > 0.7$, $\sum p_T1,2 > 1.3$ GeV^2, invariant mass cut 1.5 GeV^2 and weighting only by FDP_b the obtained statistical error would be a factor 1.95 larger than now. With the cut from SMC $\sum p_T > 2.5$ GeV^2 the error would be increased by a factor 2.25 with respect to the present situation.

5.14.3 Comparison between old and new MC tuning.

Comparing for 2002-2004 data results from previous parametrization using Sonia tuning with the new tuning we lost about 30% of the precision *i.e.* 60% *FOM*

- SONIA_TUNE: $\Delta G/G = 0.056 \pm 0.088$
- NEW_TUNE: $\Delta G/G = 0.109 \pm 0.113$

Please note that the data sample is not exactly the same as the one used for the previous release. In addition, now the new mu ID is used. Therefore, it is not surprising that the obtained results for SONIA_TUNE are not the one from the previous release note. The main reason of the precision lost is that in the new tuning contribution which describe the tails of the pT distribution, was enlarged from 0.02 to 0.04 (PARJ23) [18]. This increases contribution of LP at higher pTs. This is also the main point why the final error (0.060) is larger that expected two years ago 0.046 . In addition, 2006 data quality is worse than expected, but we gain a bit more than expected with the new region and with the usage of FL.

Here is also a good place to make a short comment about HERMES analysis of $\Delta G/G$ recently published in [37]. The results is $\Delta G/G = 0.049 \pm 0.034 \pm 0.010^{-0.099}_{+0.126}$. Citation from section 6.5 "The statistical precision of the HERMES results is the best currently available. The COMPASS results for high-pT hadron pairs in the region $Q^2 < 1$ GeV^2 has almost twice the statistical uncertainty but more data has been taken".

In the appendix B of the cited paper one finds a list of **41** parameters tuned in PYTHIA. The list does not contain the parameter PARJ23 described above. After reading the paper one can even deduce why this parameter is not there. Citation "The tuning of the fragmentation parameters was performed using a subsample with $pT < 0.8$ GeV and $Q^2 > 1$ GeV^2 where DIS process is dominant and NLO corrections are small". For the highest used pT *i.e.* 0.8 GeV the contribution from the tails of the Gaussian distribution is only about 2%. Therefore the sample used in the tuning is simply insensitive for PARJ23.

Now in the COMPASS case the change of PARJ23 from 0.01 to 0.04 increased the statistical error by a factor of about 1.5. At the same time data/MC description was improved from having a slope which reached 1.4 at $pT = 2$ GeV to a flat one. Now looking on the figure 11 in the HERMES paper the ratio between MC and data (inverse convention than in COMPASS) changes from **0.8** at $p_T = 0.7$GeV to **0.15!** at p_T=2 GeV, which makes a slope which reaches **5** in DATA/MC comparison.

[18] default is 0.01

5.15 Summary of the systematic contributions.

The systematic contributions are summarized in the Table 12. The resulting systematic error is by 10% larger than the statistical one. In addition the systematic error was evaluated in each bin of x_G the results are presented in the same table.

	total	$x_G < 0.10$	$0.1 < x_G < 0.14$	$x_G > 0.14$
$\delta(\Delta G/G_{NN})$	0.010	0.010	0.010	0.010
$\delta(\Delta G/G_{MC})$	0.045	0.077	0.067	0.129
$\delta(\Delta G/G_{f,P_b,P_t})$	0.004	0.007	0.007	0.010
$\delta(\Delta G/G_{false})$	0.025	0.030	0.021	0.016
$\delta(\Delta G/G_{A1^d})$	0.015	0.021	0.014	0.017
$\delta(\Delta G/G_{formula})$	0.035	0.026	0.039	0.057
TOTAL	0.065	0.090	0.082	0.144

Table 12: Summary of the major systematic contributions.

References

[1] *LEPTO*, http://www.isv.uu.se/thep/lepto.

[2] *JETSET*, `http://home.thep.lu.se/~torbjorn/Pythia.html`, `http://home.thep.lu.se/~torbjorn/jetset/pythia57_98dec.ps`.

[3] *POLDIS*, A. Bravar, K. Kurek, R. Windmolders, Comput.Phys.Commun.105:42-61,1997.

[4] K. Kurek, in high p_T elog 59, `http://lxfsrb6103.cern.ch/elog/High_pt/59`.

[5] SMC,B. Adeva et al. Phys.Rev.D70:012002,2004.

[6] Sonja Hedicke. *Determination of the gluon polarisation in the nucleon using hadron pairs with high transverse momentum at COMPASS*, Albert-Ludwigs-Universitt Freiburg, November 2005

[7] Sonja Hedicke. *Analysis Meeting*, November 2005.

[8] K. Kowalik, E. Rondio, R. Sulej, K. Zaremba, Acta Phys.Polon.B32:2929-2946,2001. R. Sulej, K. Zaremba, K. Kurek, E. Rondio, Measur.Sci.Tech.18:2486-2490,2007.

[9] Jean-Marc Le Goff, *COMPASS note 2004-3*

[10] J"org Pretz, *COMPASS note 2004-11*

[11] *PHAST*, http://ges.home.cern.ch/ges/phast/index.html.

[12] Stability website **http://wwwcompass.cern.ch/compass/software/offline/input/stab/index.html**

[13] Konrad Klimaszewski. *Analysis Meeting*, November 2011.

[14] Konrad Klimaszewski. *Analysis Meeting*, November 2006.

[15] *COMGEANT*, http://valexakh.web.cern.ch/valexakh/wwwcomg/index.html.

[16] *CORAL*, http://coral.web.cern.ch/coral.

[17] Vadim Aleksakin. *MC Meeting*, November 2006, /afs/cern.ch/compass/delivery/simevt/beam/beam_from_data/beam_report.pdf.

[18] Beata Pawlukiewicz. *Analysis Meeting*, December 2006.

[19] Luis Silva on behalf of the High p_T Group. *Analysis Meeting*, March 2010.

[20] Vadim Alexakhin. *Analysis Meeting*, March 2006.

[21] Konrad Klimaszewski. *Analysis Meeting*, January 2008.

[22] Beata Pawlukiewicz. *Analysis Meeting*, August 2007.

[23] A.D. Martin, W.J. Stirling, R.S. Thorne, G. Watt, Eur.Phys.J.C63:189-285,2009.

[24] *LHAPDF*, `http://projects.hepforge.org/lhapdf/`

[25] B. Andersson, G. Gustafson, G. Ingelman, T. Sjostrand, Phys.Rept.97:31-145,1983.

[26] Luis Silva on behalf of the High p_T Group. *Analysis Meeting* and *Collaboration Meeting*, June 2010.

[27] Sebastien Procureur. *Détermination de la polarisation des gluons dans le nucléon par la production de hadrons a grande impulsion transverse a COMPASS* Universite Paris XI, U.F.R. Scientifique d'Orsay, Paris, March 2006

[28] Marcin Stolarski. *Spin structure of the nucleon at low x and low Q^2 in the COMPASS experiment at CERN*, Faculty of physics, Warsaw University, Warsaw, 2006

[29] Franco Bradamante. *Analysis Meeting*, October 2010.

[30] COMPASS, M. Alekseev *et al*. Phys.Lett.B676:31-38,2009

[31] Florian Robinet, Jean-Marc Le Goff, *COMPASS note 2007-8*

[32] HERMES, A. Airapetian *etal*. Phys.Lett.B684:114-118,2010.

[33] Marcin Stolarski. *Analysis Meeting*, November 2008.

[34] COMPASS, M. Alekseev *et al*., EPJ C52 (2007) 255-265

[35] J. Hannes, Comp. Phys. Commun. 86 (1995) 147–161

[36] GRS, M. Gluck *et al*., Phys. Rev. D54 (1996) 5515–5522

[37] HERMES, A. Airapetian *etal*. arXiv:1002.3921v1 [hep-ex].

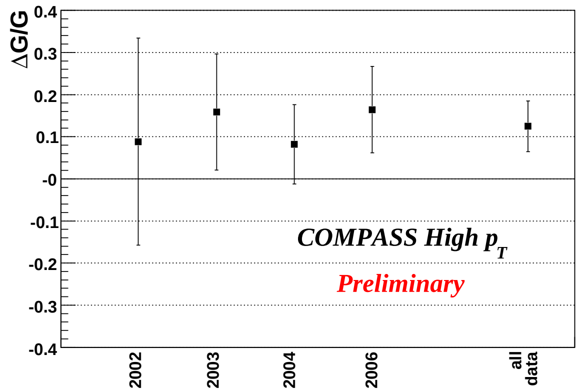

Figure 28: Final $\Delta G/G$ results for all data.

	$0.041 < x_G < 0.120$	$0.059 < x_G < 0.170$	$0.107 < x_G < 0.269$
Total	0.147 ± 0.091	0.079 ± 0.096	0.185 ± 0.165
$< x_G >$	$0.070^{+0.050}_{-0.029}$	$0.100^{+0.070}_{-0.041}$	$0.170^{+0.099}_{-0.063}$

Table 13: $\Delta G/G$ values in three bins of x_G.

6 Material proposed for release.

Final value of $\Delta G/G = 0.125 \pm 0.060 \pm 0.063$, averaged at $x_G = 0.09^{+0.08}_{-0.04}$.

The $\Delta G/G$ value for all data is illustrated in Fig. 28.

The $\Delta G/G$ value for all data in bins of x_g is given in Table 13.

Total number of events used for $\Delta G/G$ evaluation (all years): 7306932.

Table 14 containing the contributions to the systematic error.

	total	$x_G < 0.10$	$0.1 < x_G < 0.14$	$x_G > 0.14$
$\delta(\Delta G/G_{NN})$	0.010	0.010	0.010	0.010
$\delta(\Delta G/G_{MC})$	0.045	0.077	0.067	0.129
$\delta(\Delta G/G_{f,P_b,P_t})$	0.004	0.007	0.007	0.010
$\delta(\Delta G/G_{false})$	0.019	0.023	0.016	0.012
$\delta(\Delta G/G_{A1^d})$	0.015	0.021	0.014	0.017
$\delta(\Delta G/G_{formula})$	0.035	0.026	0.039	0.057
TOTAL	0.065	0.090	0.082	0.144

Table 14: Summary of the major systematic contributions.

Table 15 with the mean values of a_{LL}s and Rs.

The validation plots for the NN (Figs 29and 30).

Kinematic and hadronic distributions of all used data, Figs. 31 and 32.

Data-MC comparison plots for inclusive (Fig. 33) and for high p_T samples (Figs. 34, 35 and 36).

$\Delta G/G$ plot containing the new COMPASS high p_T measurement together with results of several experiments, Fig. 37.

$\Delta G/G$ plot containing the new COMPASS high p_T measurement in 3 x_g bins together with results of several experiments, Fig. 38.

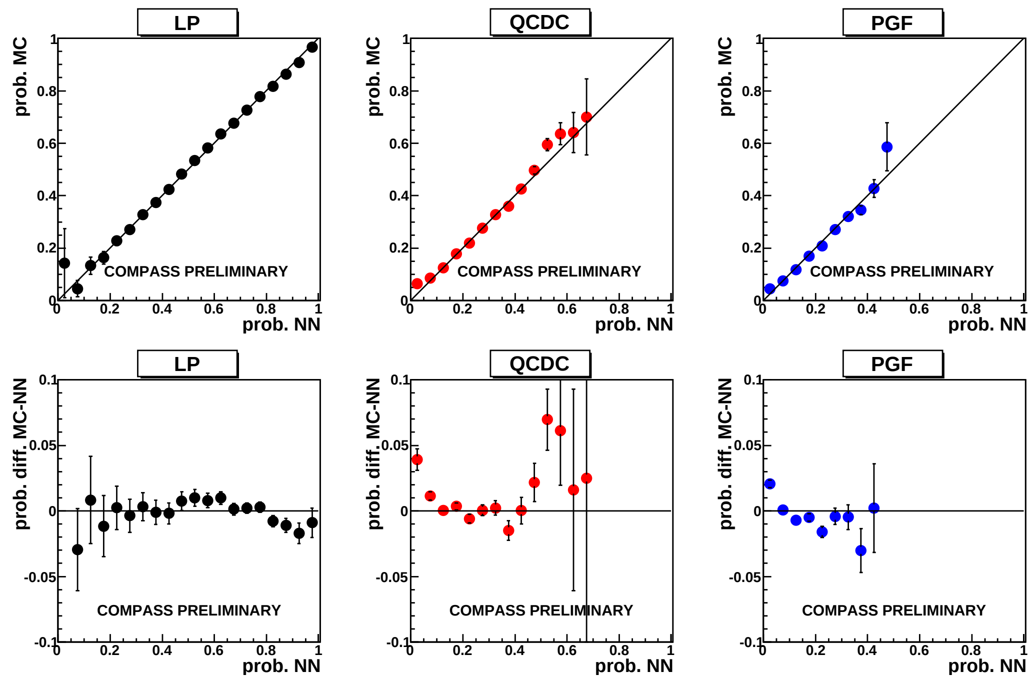

Figure 29: NN and MC comparison for R_{PGF}, R_{QCDC}, R_{LP} in bins of NN output. The lowest statistical limit for the errors is shown.

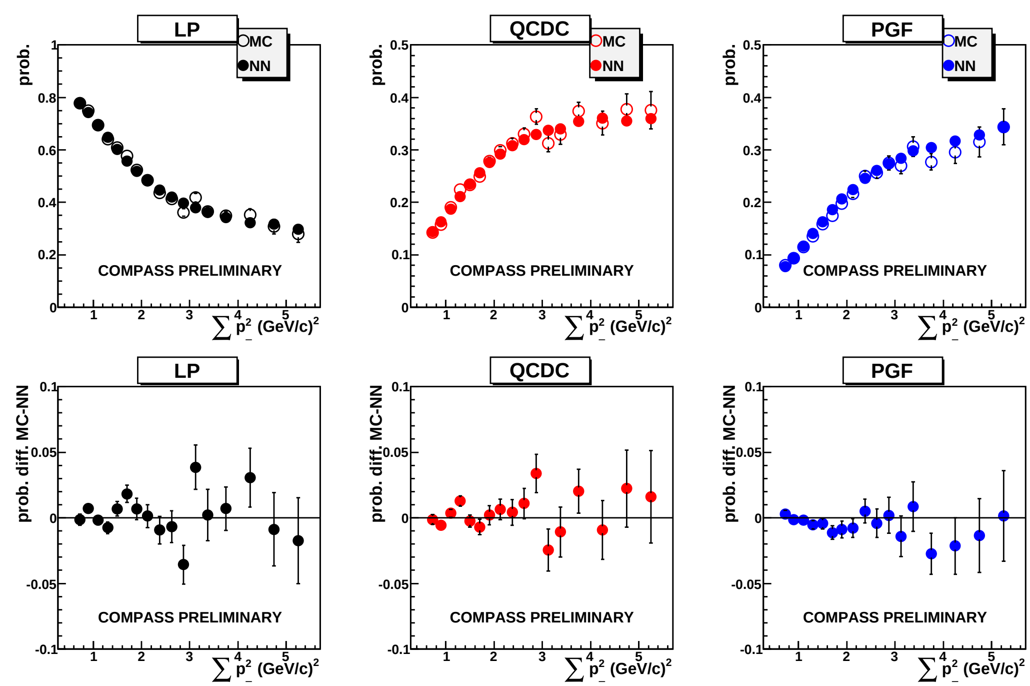

Figure 30: NN and MC comparison for R_{PGF}, R_{QCDC}, R_{LP} as a function of $\sum p_T^2$. The Lowest statistical limit for the errors is shown.

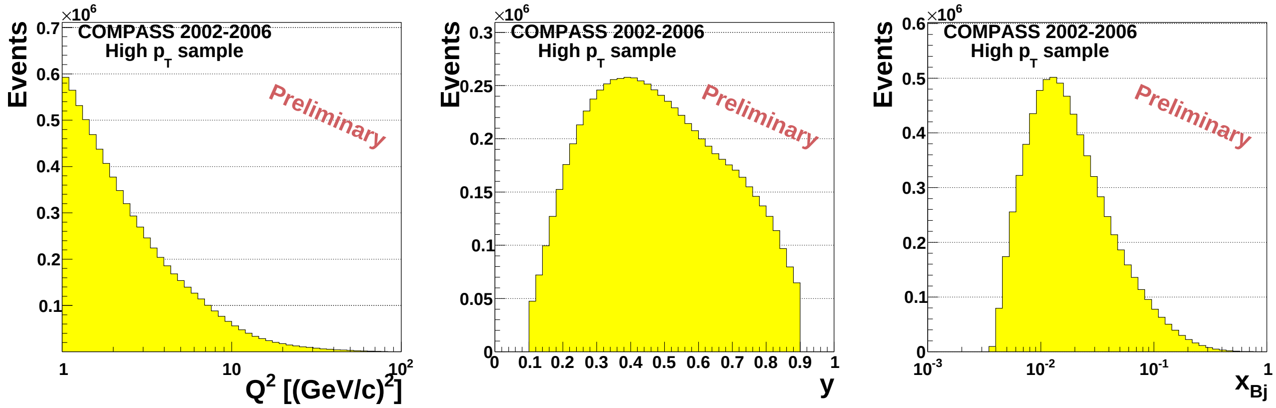

Figure 31: Q^2, y and x distributions

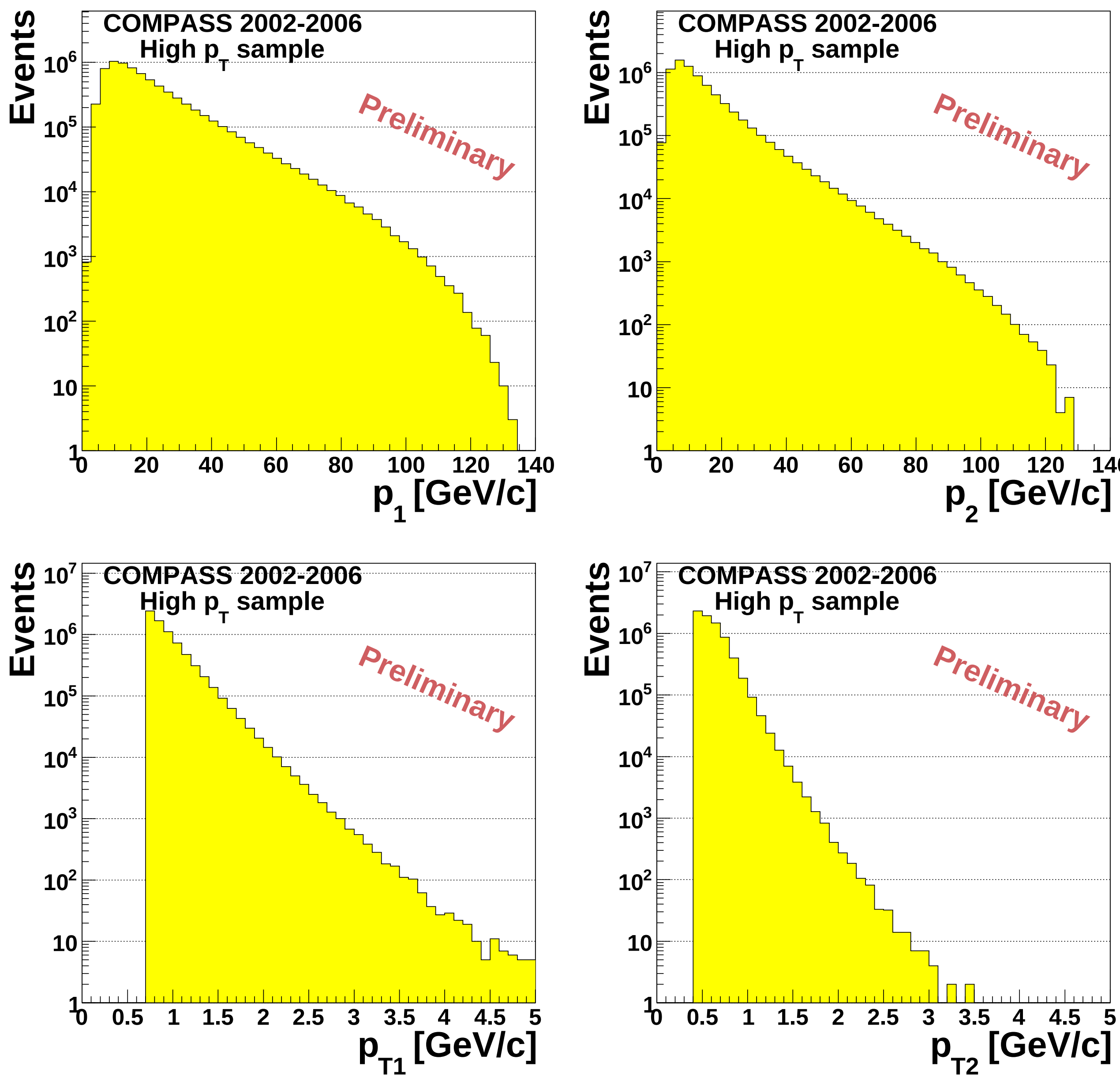

Figure 32: p and p_T for leading and sub-leading hadrons: The left column shows the leading hadrons and the right column the sub-leading one. In the first row the momenta are plotted, in the second row the transverse momenta are shown.

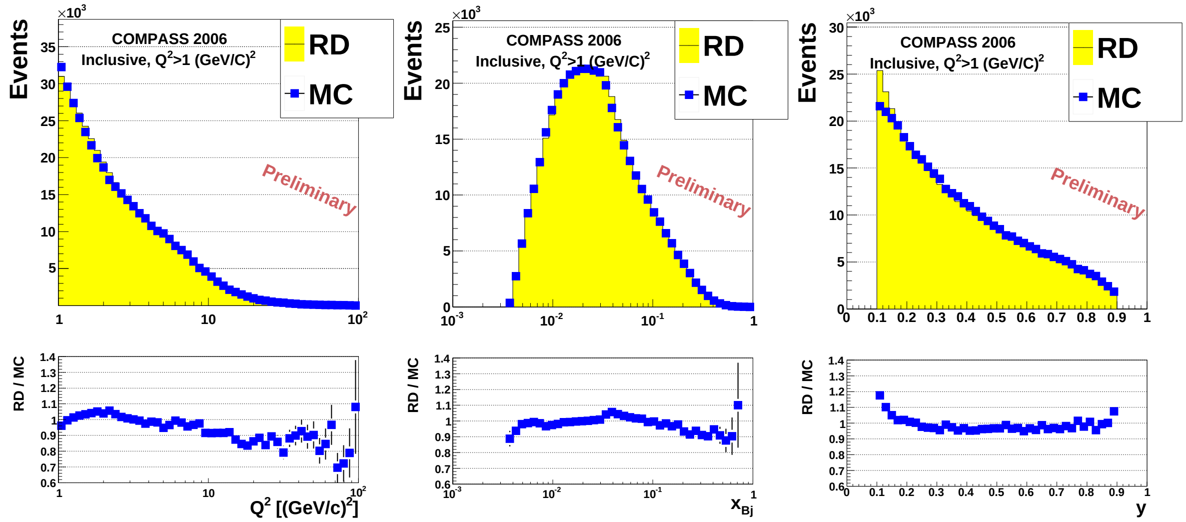

Figure 33: Kinematic distributions and data–MC comparison for 2006 inclusive sample.

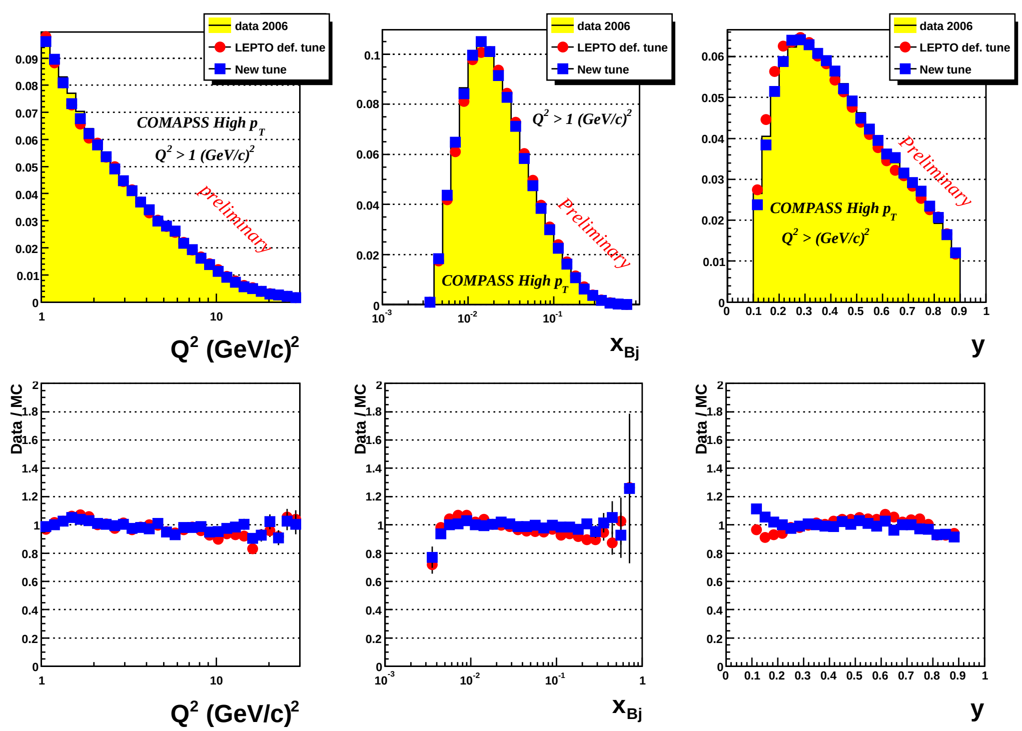

Figure 34: Kinematic distributions and data–MC comparison for 2006 high p_T sample.

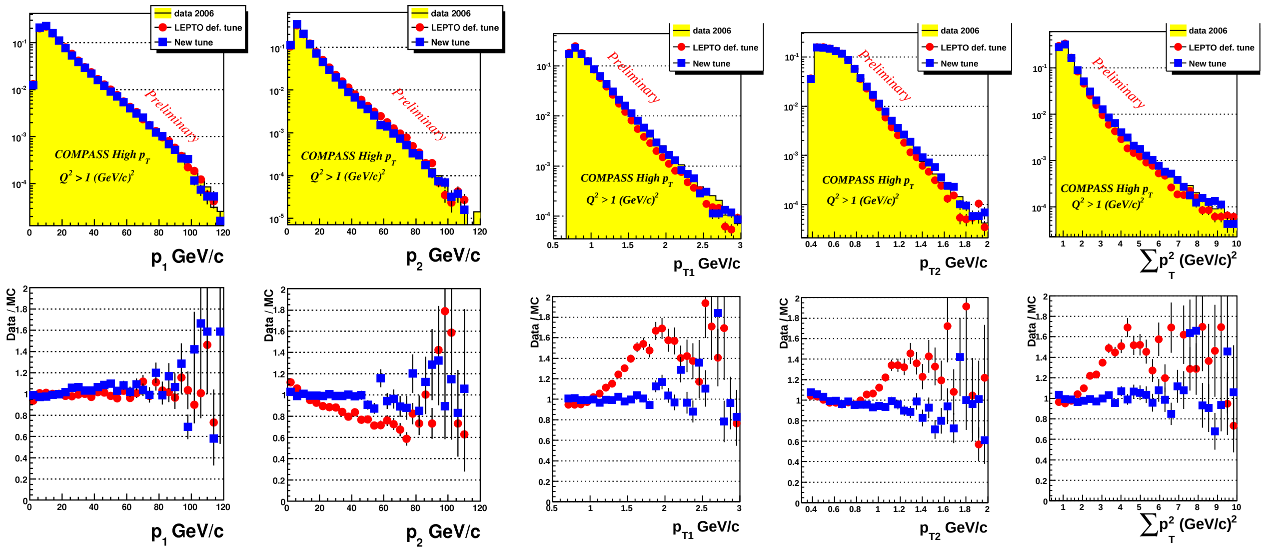

Figure 35: Hadronic distributions and data–MC comparison for 2006 high p_T sample.

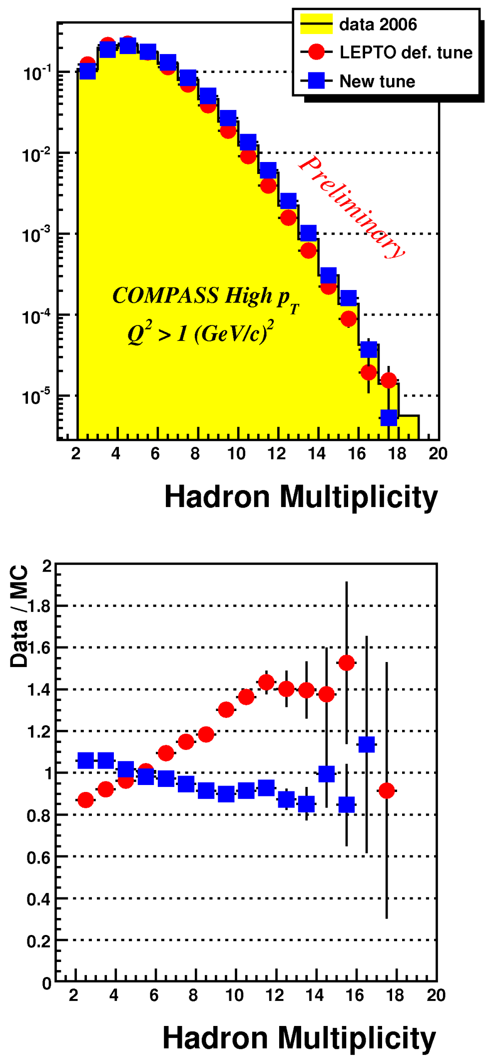

Figure 36: Hadron Multiplicity distributions and data–MC comparison for 2006 high p_T sample.

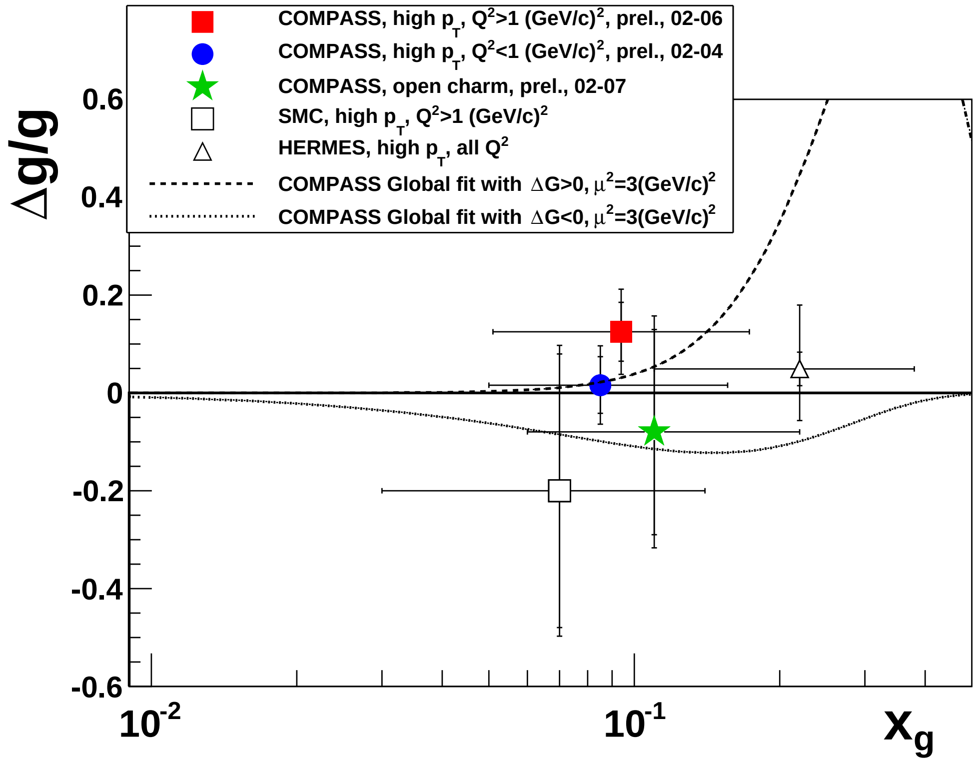

Figure 37: $\Delta G/G$ evaluated from several experiments.

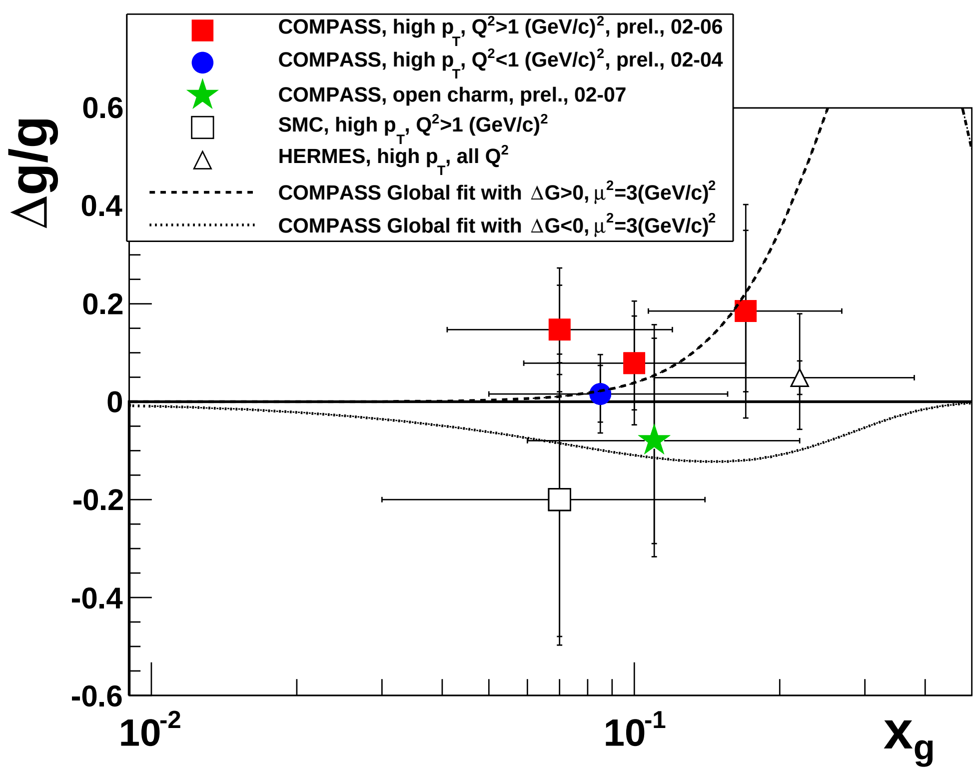

Figure 38: $\Delta G/G$ evaluated from several experiments including the new high p_T result in 3 bins.

	COMPASS PS ON MSTW08
R_{LO}	0.65
R_{QCDC}	0.21
R_{PGF}	0.14
a_{LL}^{LO}	0.49
a_{LL}^{QCDC}	0.41
a_{LL}^{PGF}	-0.32

Table 15: Mean values of analizing power,a_{LL}, and processes fractions for all MC samples.

A Appendix: Function to remove events with Middle and Inclusive Middle Triggers bits for problematic region of Middle Trigger acceptance.

```
#include "TRandom.h"
#include "TH1F.h"

/**
 * This function removes Middle Trigger and Inclusive Middle Trigger bits from
 * the trigger bit mask for events where mu' traveled through problematic
 * region of Middle Trigger acceptance in 2006 data. Rejection is based on
 * track extrapolation and gemetrical cut.
 *
 * Function expects a reference to current event and a reference to mu' track.
 */
void RemoveBadMiddleTrigger(PaEvent& e, const PaTrack& mup_tr) {
// Extract information about the Hodoscope planes once and store it in std::map for fast access
// If run number changes refresh the information
static bool first = 1;
static int run_number = 0;
static double minX = -9999;
static double Z = 0;
if(first || run_number != e.RunNum()) {
run_number = e.RunNum();
int idet;
idet = PaSetup::Ref().iDetector("HM05X1_d");
if(idet>0) {
const PaDetect& HM05 =  PaSetup::Ref().Detector(idet);
minX = HM05.Uorig() + 2.5*HM05.Pitch(); // Remove 3 strips
Z = HM05.Z();
} else {
cerr<<"RemoveBadMiddleTrigger ERROR: Detector HM05Y1_d not found!"<<endl;
exit(1);
}
first = 0;
}

if((e.TrigMask()&0x102) == 0) return;

int Npars = mup_tr.NTPar();
if(Npars == 0) {
cerr<<"RemoveBadMiddleTrigger ERROR: track does not have associated helixes!"<<endl;
return;
}
```

```
PaTPar partr = mup_tr.vTPar(Npars-1); //Track parameters in last measured point
PaTPar result;
bool res = partr.Extrapolate(Z, result, false);
if(result(1) < minX || !res) {
int new_mask = e.TrigMask() & (~0x102);
// cout<<"Old: "<<hex<<e.TrigMask()<<" New:"<<new_mask<<dec<<endl;
e.vHeader()[1] = new_mask;
}
}
```